T.C.
DOKUZ EYLUL UNIVERSITY
IZMIR INTERNATIONAL BIOMEDICINE AND GENOME INSTITUTE

TOWARDS GENERATION OF ß-TCP SCAFFOLD BASED OSTEOGENIC NICHES IN MICROFLUIDIC BIOREACTORS

İBRAHİM HALİLULLAH ERBAY

MOLECULAR BIOLOGY AND GENETICS

MASTER OF SCIENCE THESIS

İZMİR-2020

THESIS ID: DEU.IBG.MSc.2018850004

T.C.
DOKUZ EYLUL UNIVERSITY
IZMIR INTERNATIONAL BIOMEDICINE AND GENOME INSTITUTE

TOWARDS GENERATION OF ß-TCP SCAFFOLD BASED OSTEOGENIC NICHES IN MICROFLUIDIC BIOREACTORS

MOLECULAR BIOLOGY AND GENETICS

MASTER OF SCIENCE THESIS

İBRAHİM HALİLULLAH ERBAY

Supervisor: Assoc. Prof. Dr. Sinan GÜVEN

(This study is funded by TUBITAK, grant number: 118S477)

THESIS ID: DEU.IBG.MSc.2018850004

Dokuz Eylul Üniversitesi İzmir Uluslararası Biyotıp ve Genom Enstitüsü
Genom Bilimleri ve Moleküler Biyoteknoloji Anabilim Dalı,
Moleküler Biyoloji ve Genetik Yüksek Lisans programı öğrencisi
İbrahim Halilullah ERBAY **'MİKROAKIŞKAN BİYOREAKTÖRLERDE ß-TCP ESASLI DOKU İSKELELERİ KULLANILARAK OSTEOJENİK NİŞ GELİŞTİRİLMESİ'**
konulu Yüksek Lisans tezini 22.06.2020 tarihinde başarılı olarak tamamlamıştır.

Doç. Dr. Sinan GÜVEN
BAŞKAN

ÜYE
Doç. Dr. Duygu SAĞ WINGENDER
Dokuz Eylul Üniversitesi

ÜYE
Dr. Öğr. Üyesi Ozan KARAMAN
İzmir Kâtip Çelebi Üniversitesi

YEDEK ÜYE
Doç. Dr. Yavuz OKTAY
Dokuz Eylul Üniversitesi

YEDEK ÜYE
Dr. Öğr. Üyesi Cumhur H. TEKİN
İzmir Yüksek Teknoloji Ensitüsü

Dokuz Eylul University Izmir International Biomedicine and Genome Institute
Department of Genomics and Molecular Biotechnology,
Molecular Biology and Genetics graduate program Master of Science student
İbrahim Halilullah ERBAY has successfully completed his Master of Science thesis titled
'TOWARDS GENERATION OF ß-TCP SCAFFOLD BASED OSTEOGENIC NICHES IN MICROFLUIDIC BIOREACTORS'
on the date of 22/06/2020.

Assoc. Prof. Sinan GÜVEN
CHAIR

MEMBER
Assoc. Prof. Duygu SAĞ WINGENDER
Dokuz Eylul University

MEMBER
Asst. Prof. Ozan KARAMAN
Izmir Kâtip Çelebi University

SUBSTITUTE MEMBER
Assoc. Prof. Yavuz OKTAY
Dokuz Eylul University

SUBSTITUTE MEMBER
Asst. Prof. Cumhur H. TEKİN
Izmir Insitute of Technology

TABLE OF CONTENTS

LIST OF TABLES

LIST OF FIGURES

List of Abbreviations

2D	2-Dimensions
3D	3-Dimensions
ß-TCP	ß-tricalcium phosphate
µCT	Micro computed tomography
ALP	Alkaline phosphatase
BM	Bone marrow
BMMSCs	Bone marrow mesenchymal stem cells
BMP-2	Bone morphogenetic protein 2
BSP	Bone sialoprotein
EM	Electron microscopy
ECM	Extra cellular matrix
FBS	Fetal Bovine Serum
FGF-2	Fibroblast growth factor 2
HA	Hydroxyapatite
HUVECs	Human umbilical vein endothelial cells
ICC	Immunocytochemistry
IHC	Immunohistochemistry
mBM	Mouse bone marrow
MØ	Mouse macrophage
mBMMSCs	Mouse bone marrow mesenchymal stem cells
mBMMØ	Mouse bone marrow monocyte/macrophages
MTT	3-(4,5-Dimethylthiazol-2-yl)-2,5-diphenyltetrazolium bromidefor
OPN	Osteopontin

PDMS	Polydimethylsiloxane
RUNX2	Runt-related transcription factor 2
TCP	Tricalcium phosphate
VEGF	Vascular endothelial growth factor
XRD	X-Ray Diffraction

ACKNOWLEDGEMENTS

Foremost, I would like to express my gratitude to my advisor, Assoc. Prof. Sinan Güven for his continuous guidance, support, patience, mentorship, encouragement and enthusiasm while nurturing this study from start to the end.

Besides my advisor, I would like to thank Asst. Prof. Ozan Karaman and Bonegraft Co. family for their support and patience.

I thank to TUBITAK for their funding for this study.

My sincere thanks to all IBG core facilities for their help and motivation.

I thank to the all my lab members in Therapeutic Bioengineering Group: Emine Kahraman with her inexhaustible supply of hand creams, Melis Asal and her theatre performances during experiments, Olcay Burçin Akbulud and Ali Kemal Baş for their never-ending support and friendship.

I thank to all fellow students at IBG: Aleyna Eray, Yağmur Güneri, Mert Dikmenoğulları, Merve Arslan, Çağla Kiser, Hamdiye Uzuner, Resul Özbilgiç and Aslı Korkmaz for all the enjoyable time and their support.

I thank to Saniye Gül Kaya for her unconditional love, patience, motivation and continuous support in every step.

I thank all the heroes of my life, my family.

I dedicate all my efforts to the scientific community and their shining light on life, health workers and all the people who lost their lives during COVID-19 pandemic.

TOWARDS GENERATION OF ß-TCP SCAFFOLD BASED OSTEOGENIC NICHES IN MICROFLUIDIC BIOREACTORS

İbrahim Halilullah ERBAY, Izmir International Biomedicine and Genome Institute, Dokuz Eylul University Health Campus, Balcova, 35340, Izmir / Turkey

ABSTRACT

Traditional bone tissue engineering applications often aim to develop therapeutic solutions. Most of these efforts are circled around a biomaterial or composites to provide optimum results. However, reliable generation of biological properties of bone tissue engineering biomaterials suffers from the poor recapitulation of *in vivo* systems in laboratory conditions. Much of the problems stem from the variation among the individuals and poor mimicry systems. Therefore, a physiologically relevant *in vitro* system, which can provide a total mimicry of *in vivo* environment thus assist to access the dynamic behavior of osteogenic environment is needed. Dynamic systems such as microfluidic devices and bioreactors, which have already proven to be a powerful tool for biological system modeling and manipulation is a well-suited methodology to achieve such endeavor. From controlling chemical and mechanical cues to cross talk among cells to evaluate cell-material interactions, microfluidics satisfies crucial requirements for an *in vivo*-like system. Many tissue models have been reported over the past decades, nonetheless, bone tissue has been slow to catch up. The developed bioceramic here enables a tailored environment for dynamic bone co-culture platforms. In this study, a functional osteogenic niche model, which can perform bone resorption/secretion was intended. To achieve this, primary mouse bone marrow cells, a tailored biomaterial and microfluidic bioreactors was used. Building upon the dynamic co-culturing methods, this thesis discusses a simpler and robust approach to functionalize the osteogenic niche while providing an *in vivo*-like microenvironment using dynamic tools. The developed platform achieved a simple and robust manufacturing method for ß-tricalcium phosphate (ß-TCP) scaffolds using a polymeric foam replication method. And it is tailorable with any bioreactor setup, shapes and volumes with desired porosity percentages. The ß-TCP was subjected to mechanical analysis to confirm its resemblance to native inorganic bone and X-ray diffraction analysis to determine crystal structure. For osteogenic niche, freshly isolated mouse bone marrow mesenchymal stem

cells (mBMMSCs) and monocytes/macrophages (mBMMØ) was used to form basic cellular components of the bone. The osteogenic niche seeded on ß-TCP scaffold was then placed in a microfluidic bioreactor to complete the setup. Scanning electron microscopy (SEM) analysis showed that after 21 days of culture the ECM secreted by cells covered most of the scaffold volume. Moreover, real-time polymerase chain reaction (qPCR) was confirmed significant increase of osteocalcin, ALP and cathepsin-K proteins as an indication of formation of osteoblast and osteoclast cells.

Keywords: Bone Tissue Engineering, Osteogenic Niche, Microfluidic Bioreactor, Bioceramics

MİKROAKIŞKAN BİYOREAKTÖRLERDE B-TCP ESASLI DOKU İSKELELERİ KULLANILARAK OSTEOJENİK NİŞ GELİŞTİRİLMESİ

İbrahim Halilullah Erbay, İzmir Uluslararası Biyotıp ve Genom Enstitüsü, Dokuz Eylul Üniversitesi, Sağlık Kampüsü, Balçova, 35340, İzmir / Türkiye

ÖZET

Geleneksel kemik doku mühendisliği uygulamaları genellikle terapötik çözümler geliştirmeyi amaçlamaktadır. Bu çabaların çoğu, optimum sonuçları elde edebilmek için biyomalzemelerin kullanımı etrafında dönmektedir. Bununla birlikte, kemik doku mühendisliği biyomalzemelerinin biyolojik özellikleri *in vivo* sistemleri taklit etmede tek başına yetersiz kalmaktadır. Bu alandaki sorunların çoğu her bireyin birbirine gösterdiği farklılık ve bu bireylerdeki sistemleri taklit edecek sistemlerin başarısız olmasından kaynaklanmaktadır. Bu nedenle, *in vivo* ortamların toplam taklidini sağlayabilen ve osteojenik ortamın değişen davranışları hakkında bilgi sağlayabilen fizyolojik olarak uygun bir sistem gereklidir. Biyolojik sistem modellemesi ve manipülasyonu için güçlü bir araç olduğu kanıtlanmış mikroakışkan cihazlar ve biyoreaktörler gibi dinamik sistemler, bu tür bir çabaya ulaşmak için çok uygun bir metodolojidir. Mikro akışkanlar, kimyasal ve mekanik ipuçlarını kontrol etmekten, hücre-malzeme etkileşimlerini değerlendirmek için hücreler arası iletişime kadar *in vivo* benzeri bir sistem oluşturmak için önemli gereksinimleri karşılar. Son on yılda birçok doku modeli rapor edilmiştir, buna rağmen kemik dokusu bu alanda geride kalmıştır. Bu çalışmada geliştirilen biyoseramik, dinamik kemik ko-kültür platformları için özel bir ortam sağlamaktadır. Bu çalışmada, kemik rezorpsiyonu / sekresyonu gerçekleştirebilen fonksiyonel bir osteojenik niş modelinin geliştirilmesi amaçlanmıştır. Bunu başarmak için, uyarlanmış seramik biyomalzemeler, mikroakışkan biyoreaktörler ve primer fare kemik iliği hücreleri kullanılmıştır. Dinamik ko-kültür yöntemlerine dayanan tez, dinamik araçlar kullanarak *in vivo* benzeri bir mikro-ortam sağlarken osteojenik nişin işlevselleştirilmesi için daha basit ve güçlü bir yaklaşımı da tartışmaktadır. Geliştirilen platform, polimerik köpük replikasyonu yöntemi kullanılarak ß-trikalsiyum fosfat (ß-TCP) yapı iskeleleri için basit ve verimli bir üretim yöntemi ile elde edildi. Üretilen iskele, herhangi bir biyoreaktör düzeneğine göre istenen gözeneklilik

yüzdelerinde ve istenen geometride üretilebilmektedir. Doku iskelesine, üretim öncesi ve sonrası kristal yapıyı belirlemek için X-ışını kırınım analizi yapıldı. İskelenin kemiğin doğal yapısına benzerliğini doğrulamak için mekanik analize tabi tutuldu. Osteojenik niş için, proje kapsamında izole edilmiş fare kemik iliği mezenşimal kök hücreleri (mBMMSC'ler) ve monosit/makrofajlar (mBMMØ), kemiğin temel hücresel bileşenlerini oluşturmak için kullanıldı. Daha sonra ß-TCP iskelesine ekilen hücreler ile birlikte oluşan osteojenik niş, mikroakışkan biyoreaktöre yerleştirildi. Tarama elektron mikroskobu (SEM) analizi, 21 günlük kültür sürecinden sonra hücreler tarafından salgılanan ECM'in iskele hacminin çoğunu kapsadığını göstermiştir. Ayrıca, gerçek zamanlı polimeraz zincir reaksiyonunun (qPCR), osteoblast ve osteoklast hücrelerinin oluşumunun bir göstergesi olarak osteokalsin, ALP ve katepsin-K proteinlerinde önemli bir artış olduğu doğrulandı.

Anahtar sözcükler: Kemik Doku mühendisliği, Osteojenik Niş, Mikroakışkan Biyoreaktör, Biyoseramik,

1 SCOPE OF THESIS

1.1 Motivation

Historically, bone tissue engineering has been focused on developing better implants or grafts for enhanced bone regeneration[1]. Over the last decade, the focus has been shifted into engineering *in vitro* models to carefully study the physiology and pathology[2]. The consensus strategy to develop such a model consists of several steps. These steps include i) manufacturing a biomaterial to serve as the tissue scaffold, ii) seeding cells on the scaffold, iii) culturing the cells for a period of time, and iv) analyzing the structure. For the first step, plenty of polymers, ceramics, and composite materials have been studied and are available in the literature. The advantage each type offers is also bringing undesired disadvantages that may fail the ultimate goal. For instance, polymers offer tunable properties and reproducibility, while biodegradation can cause toxicity[3]. Additionally, many chemical or physical alterations are made to tailor an ideal scaffold, such as the addition of ceramic particles to polymer networks. Biomaterial research has brought a cascade of selection options, which can be overwhelming and often fail to deliver basic clinical needs. The main reason behind this is the primary focus of many studies is to add a component ‘’a.’’ to a known biopolymer and evaluate the cellular response. One can use combinations of several additives on different polymers and conduct many studies, none of which will significantly contribute to the field[4]. The same approach can be seen in ceramic materials, as many different ceramics are studied to the atomic level with different additives, which allegedly increase osteoinductivity[5]. Concerning biomaterial research, properties of materials including mechanical, chemical, physical, and biological properties are vast and may not be advantageous for a bone model study to try to tailor each individually. For the second step, several strategies are used. These include the utilization of cell lines, primary cells harvested from either human or mice or *in vivo* implantation of the scaffold prior the *in vitro* seeding and culture. For the third step, tissue engineered cell-material construct is cultured statically or dynamically in an *in vitro* platform. The usage of dynamic systems such as microfluidic devices allows a better recapitulation of *in vivo* environments. Finally, the cultured construct is often analyzed by qPCR, electron microscopy (EM), micro-computed tomography (μCT), immunohistochemistry (IHC), and immunocytochemistry (ICC).

As bone is perhaps the most heavily studied tissue, each of these steps is expanded to encompass many disciplines[6]. Nonetheless, currently, there is no functional bone tissue model that can allow studying neither physiology nor pathology[7]. Although there is an avalanche of reasons as one try to understand, the complexity of bone challenges scientists to succeed. Moreover, engineered bone tissue models often lack the complexity of the native microenvironment in terms of structural hierarchy, vascularization, and cellular composition[8]. Bone regeneration and cellular dynamics are highly dependent on the non-immunological regulatory roles of macrophages/monocytes, which are often neglected. In this context, we developed a ß-TCP based scaffold for 3D dynamic culture systems including bioreactors and microfluidic systems that are aimed to model an osteogenic niche that can perform bone secretion and resorption. Generation of the osteogenic niche relied on culturing primary bone marrow cell-laden scaffolds.

The model holds the potential to allow cell-cell interactions and bone remodeling process in a simplified dynamic microfluidic chamber, which might improve the current view of *in vitro* bone models. Such a system might be useful for therapeutic tools for many bone diseases, close investigation, and experimentation for osteogenic niche cross talks and processes. Moreover, the system may allow alterations in bone regulation and repair mechanisms using additional tools. Overall, system developed in this thesis study holds promise for a high-performance functional tissue platform.

1.2 Objectives

1.2.1 Objective 1

The first objective was to manufacture the bioceramic scaffold from β-TCP using a foam replication method (Fig. 1). Tailoring a bioceramic was a necessary step since it profoundly affects the overall performance of the tissue formed and offers better suitability than the commercial products[9]. However, it may also be problematic to decide which properties are to be tailored. To allow cellular migration, the construct should be porous[4]. Nonetheless, the shape, diameter and distribution of these pores are of importance since they will be affecting the cellular proliferation. Besides, tailoring the pore structure is closely related to the particle size and sintering regime. Furthermore, the mechanical properties such as compressive strength

and stiffness are other parameters that must be taken into consideration while tuning the porosity[5]. After considering all these factors, we decided to use β-TCP since it is balanced in terms of absorption, degradation and new bone formation while preserving stability due to the calcium (Ca^{2+}) and sulfate (SO_4^{2-}) ion release, which are essential for de novo bone formation. Moreover their chemical similarity to the inorganic part of the bone and being non-toxic, biocompatible and most importantly bioactivity makes it one of the best choice for bone tissue engineering applications[10], [11]. More importantly, the physicochemical interaction between native bone and the ß-TCP is known to be osteoconductive, which supports osteoblastic differentiation, adhesion and proliferation on the scaffold. Nonetheless, reproducibility of bioceramics is cumbersome and, disturbance of the cell-scaffold structure is often necessary to analyze the structure after the culture period[12], [13]. Namely, after the establishment of the osteogenic niche, the structure needs to be characterized, however, the analysis methods available often require irreversible disturbance of the niche-scaffold setup. Therefore, a new scaffold with new cells needs to be prepared for further experimentation and naturally the new construct will have significant differences with the previous system. In this context we provide several strategies and suggestions to overcome such limitations.

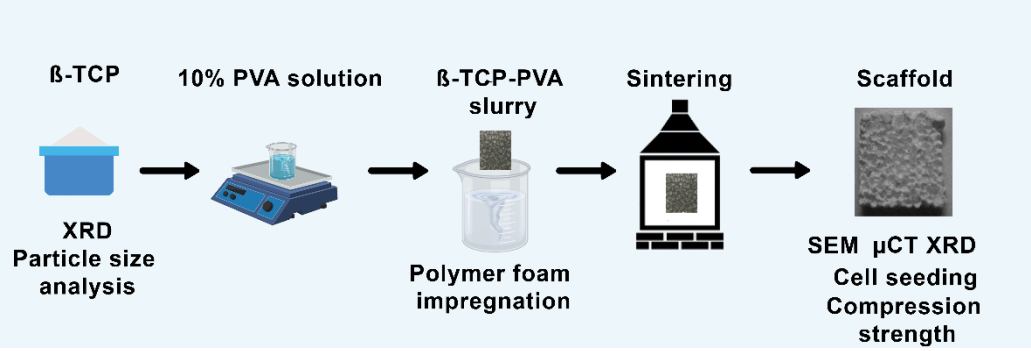

Figure 1. Scaffold fabrication pathway. The ß-TCP powder is grinded and mixed with 10 % PVA binder solution. Later the laser cut polymeric foams are immersed to the solution in a pressure chamber. Further, the green body is dried and sintered to obtain the final structure.

1.2.2 Objective 2

Another objective was the manufacturing of a microfluidic bioreactor. Traditional 2D monolayer static cell culture methods do not accurately represent the cell organization in an *in vivo* microenvironment[14]–[16]. Moreover, such systems fail to recapitulate the complex

physiological and mechanical microenvironment. Therefore, a total *in vivo*-like model with physiologically relevant cues for cellular growth and proliferation is hindered[17]. Especially, mechanical stimulation in developed models both 2D and 3D is often not included, which profoundly affect cellular response and overall success of the model[7]. Dynamic systems such as microfluidics and bioreactors, can be utilized for many biomaterial types such as porous ceramics or hydrogels. Moreover, these systems can be incorporated with pumps or valves to introduce additional shear stress to the model allowing modeling a more *in vivo*-like system[18]–[21]. Previously, such setups often utilized single cell types with simpler designs. Current models on the other hand, exhibit complex design parameters and co-culture of different cell types seeded in various types of biomaterials are utilized. Such systems allow recreation of complex tissues and tissue interfaces and studying multiple functions on a single model[22]–[24]. Moreover, usage of laminar flow also allowed fluidic manipulations to create concentration gradients in the system which added another layer of natural environment recapitulation[21], [22]. In terms of methodology to manufacture such devices received increased attention causing various different techniques and protocols for a device that fits best for any application with precise control on the microenvironment[25]. In this context, we designed and manufactured a polymethyl methacrylate-based microfluidic device that can the dynamic culture environment and open for implementation of *in situ* analyses. After obtaining cell-scaffold construct, the scaffold is press-fitted into the microfluidic device and a syringe pump is used to supply cell culture medium at a specific flow rate (Fig. 2).

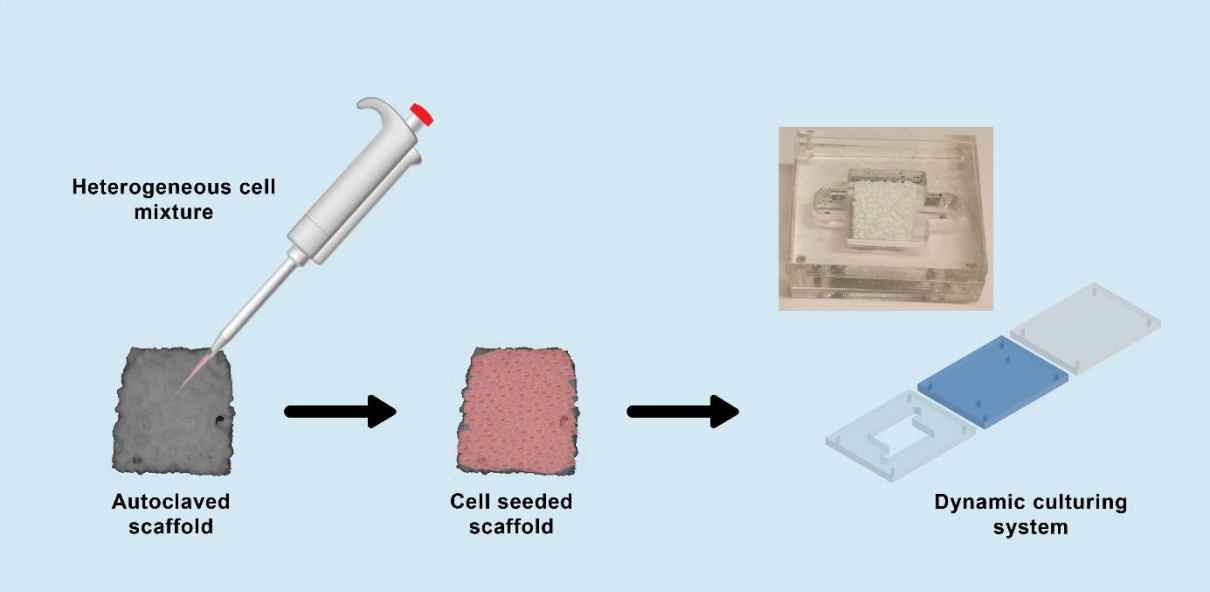

Figure 2. 3D dynamic environment setup. After manufacturing of the ß-TCP scaffold and sterilization, harvested cells are seeded on the scaffold. Later, the scaffold is placed in a press-fit chamber in a dynamic setup. The system is then supplied with culture medium at a specific flow rate.

1.2.3 Objective 3

In order to obtain a functional method, the system should closely resemble *in vivo* microenvironment. Tissue engineering studies often require proper selection of the cell source, which significantly affects the outcome[26]–[29]. Whether autologous, allogenic or xenogenic, depending on various factors selection of the cell source may vary. For instance, if the generated model to be implanted, autologous cells are the most suitable source because of near no rejection rate after implantation. However, as difference in cell source to the implantation site increase for instance in case of a xenogenic source, the immune response becomes impossible to prevent[30]. In this study, implantation is not a direct objective and therefore, such issues are ignored. However, for the model's success, primary cells are the best option[7]. Therefore, we decided to use primary bone marrow cells since it can provide both osteoblast and osteoclast precursor cells and easier to adapt for osteogenic differentiation[31]–[33]. We used primary mouse bone marrow cells, which were further sorted to mesenchymal stem cells and monocyte derived macrophages (Fig. 3).

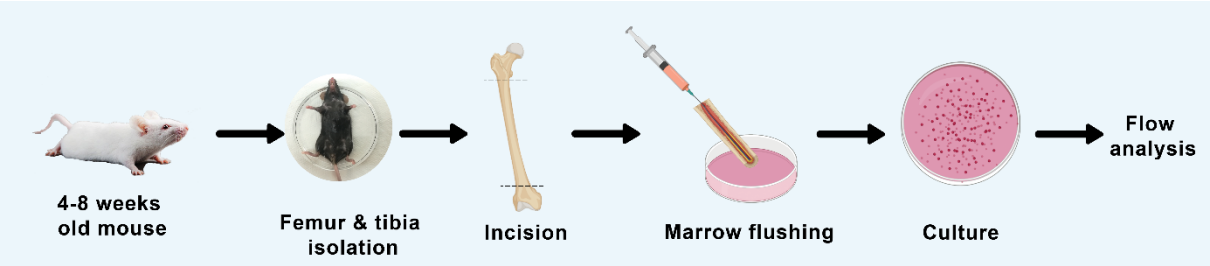

Figure 3. Cell isolation procedure. 4-8 weeks old mice were sacrificed, and their femur and tibia were isolated. Later, the bones were incised, and the marrows were flushed. After culturing of the harvested cells, flow cytometry analysis was used to identify cell populations.

1.3 Hypothesis

In this thesis study, we hypothesize that a dynamic microenvironment is one of the key factors for modeling a functional osteogenic niche and conventional static cell culture methods is insufficient to fulfill this aim. Further, monocyte/macrophage derived osteoclasts and MSCs derived osteoblasts can allow formation of a functional bone unit that can resorb and secrete bone tissue.

2 INTRODUCTION

2.1 The osteogenic niche

The osteogenic niche is the concept of a physical entity that consists of osteoprogenitors, pre- and mature osteoblasts, osteocytes and osteoclasts[34]. The niche represents a local tissue microenvironment that maintains and regulates the osteogenic processes. Together, they form a multifunctional tissue that plays a role in mechanical support of the body and protection, mineral homeostasis and endocrine functions[35]–[37]. The bone formation, also known as ossification, is the process of bone synthesis, which begins in the third month of a fetus in humans and continues by late adolescence. Once the bone tissue formation is completed, the tissue is remodeled throughout life[38]. Bone remodeling is a continuous and dynamic process, which involves bone resorption by osteoclasts and new bone formation by osteoblasts (Fig. 4). Resorption and formation of bone are performed in a balanced homeostatic equilibrium between osteoblasts and osteoclasts. The process is controlled by various local factors such as growth factors and cytokines and systemic factors including calcitonin and estrogens and finally osteocytes, acting as mechano-sensors[39], [40]. The key events can take several remodeling signals such as calcium ion dissociation from the bone matrix, bone initiatory growth factor release via osteocyte due to a mechanical strain on the bone or hormones[8], [41]–[43]. After the activation phase, osteoblasts, which have differentiated from mesenchymal precursors, recruit osteoclast precursors that are differentiated from macrophages/monocytes to the site. Later, osteoblasts induce osteoclastogenesis to which results in multinucleated osteoclasts to start the resorption phase. During resorption, osteoclasts isolate the site and pump hydrogen ions, creating an acidic zone to resorb the mineralized bone. Moreover, the remaining organic bone matrix is degraded by the release of cathepsin K, which is a collagenolytic enzyme. Following the resorption, the collagen remnants are removed, and the formation phase is initiated where osteoblasts secrete new bone matrix, which is a combination of type I collagen and hydroxyapatite (HA) with other salts. Once the bone matrix formation is completed, a number of osteoblasts remain entrapped in the bone as osteocytes and others flatten to cover quiescent bone surfaces as bone lining cells while the rest die by apoptosis[44]–[50]. Bone remodeling process relies on dynamic interactions and equilibrium among osteogenic niche cells. A disruption in these interactions leads to bone pathologies, often difficult to treat.

Therefore, it is important to elucidate the complete interactions among the key players and their regulation to benefit better therapeutics.

Figure 4. The bone remodeling process is a continuous cycle of bone resorption by osteoclasts

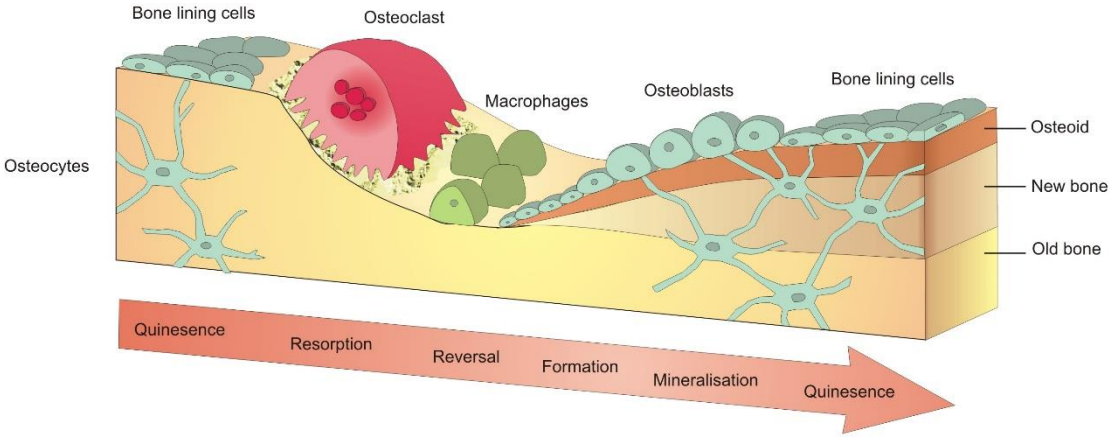

and formation of new bone tissue by osteoblasts. Later, the osteoblasts can differentiate into osteoids and stay in the calcified tissue. The cycle may be initiated by several factors such as damage[51].

2.2 Biomaterials for bone tissue engineering

Tissue engineering applications investigate biological tissues in the hope of creating therapeutic solutions for diseased or damaged tissues and organs[52]. The basic strategy of the principle is to use stem cells and biomaterials to form an *in vitro* engineered tissue[53]–[55]. Further, the constructed tissue is either implanted for therapeutic purposes[56]–[59] or further investigated to elucidate cellular mechanisms[7], [60]–[64] and possible drug discoveries[65]–[68]. The role of the biomaterial is to provide cells a scaffold on which new tissue can be constructed. Over the decades, numerous natural and synthetic materials have been investigated, and their performance reviewed, for each tissue, one can find thousands of different materials and their chemically or physically altered, biomolecule impregnated and composite forms[17], [69]–[72]. From the material point of view, properties of materials, including mechanical, chemical, and biological properties, are of importance for this purpose. Therefore, material selection, design, and manufacturing processes are dependent on the type of tissue[54].

Bone is a hard tissue and provides mechanical support to the body. Although the bone remodeling process can allow self-healing in bone tissue, as the defect size increases, the mechanism fails to heal the defect[73], [74]. These defects disrupt the biomechanical balance and can lead to severe damages. To tackle this problem, the defect is often filled with biomaterials to serve as a scaffold for cells to proliferate and form new tissue[75]. On the other hand, if the defect size is too large to be restored, the tissue replacement surgery is performed[76]–[78]. Ideally, the biomaterial should not induce a robust immune response and provide mechanical stability to the site[79]. Further, if the defect is within the range for assisted healing, the biomaterial should eventually be replaced by new tissue and therefore, must be resorbable for ideal results[80]. Moreover, cell adherence, proliferation, and ingrowth should be favorable to allow new tissue formation[81]. All together, these restrictions provide a baseline for material selection. Since the variability of defect characteristics is high, numerous biomaterials are widely used, including metals, polymers, ceramics, and composites[82], [83]. Frequently used biomaterials for bone tissue engineering are listed in Table 1.

Table 1. Biomaterials frequently used in bone tissue engineering

Biomaterials	Characteristics	Advantages	Disadvantages	Reference
Natural bone	~60 % Inorganic mostly HA ~23 % Protein mostly collagen ~9 % Water			[84], [85]
Titanium and titanium alloys	High corrosion resistance Consistent modulus of elasticity with natural bone	Good osseointegration	Non-degradable	[86], [87]
Magnesium	Porous Biodegradable	Consistent mechanical properties with natural bone Biodegradable	Ion toxicity or particle leaching risk	[88], [89]
Gelatin	Denatured collagen	Forming 3D structure by cross-linking	Poor mechanical properties	[90]–[93]
Silk fibroin	Fibrous protein	Tunable biodegradation	Low osteogenic capacity	[94]–[97]

Collagen	Forming organic part of natural bone	Biodegradable	Swelling Poor mechanical properties	[73], [98]–[101]
PCL	Synthetic Biocompatible	Injectable	Slow degradation rate Poor cell adhesion	[102], [103]
PVA	Synthetic Biodegradable	Flexible characteristics e.g. porosity, shape and degradation rate	Poor cell adhesion	[104], [105]
HA	Forming inorganic part of natural bone	Osteoconductive Non-toxic No rejection		[98], [106]–[108]
TCP	Close Ca/P ratio to natural bone	New tissue can benefit from calcium and phosphorous Biodegradable		[80], [109]–[111]
Bioactive glass	Composed of Na_2O, CaO, SiO_2 and P_2O_5	Activates osteogenesis Bonds strongly to hard and soft tissue	Brittleness	[112]–[115]

2.3 Perfusion bioreactors for bone tissue engineering

Traditional approaches for bone tissue engineering often require high cell number to be seeded on a scaffold to succeed. However, expansion of cell in *in vitro* conditions at a 3D setup suffers from nutrient transfer limitations which lowers the feasibility of the application[116]. Bioreactor systems emerge as a solution improving the culture media circulation and convective transport of nutrients in the structure. In addition to the mass transport benefit, bioreactors allow controlling and monitoring of environmental conditions including pH, O_2 and CO_2 concentrations in the system[117]. Further, the shear stress created by the fluid flow also contributes to the mechanical stimulation sensed of cells in the structure. This stimulation is particularly important in bone tissue engineering applications due to the increase in production

of alkaline phosphatase (ALP), collagen type I and mineralization of osteoblasts[118], [119]. In the natural bone, mechanical loading influences the cell lining in lacunar and canalicular spaces and results in differentiation and proliferation[120]. Therefore, bioreactors provide significant benefits for such applications. Over the years, this strategy has been proved to be effective to obtain higher cell densities, improve cell seeding efficiency, cell proliferation, contamination risk and MSC to osteoblast differentiation[118], [121]. For instance, as Wendt *et al.* reported, that cell seeding of 3D scaffolds by continuous perfusion significantly enhanced cell uniformity and number of viable seeded cells compared to static cultures[122]. Moreover, due to the matrix secretion in bone cells, static conditions create an oxygen gradient depleting in the core of the scaffold thereby causing cell death[123]. Bioreactors have been shown to overcome this problem, hence providing greater cellular viability. Generally, four types of bioreactors in bone tissue engineering are often used which are spinner flasks, rotating wall bioreactors, hollow-fiber bioreactors and perfusion systems (Fig. 5)[117].

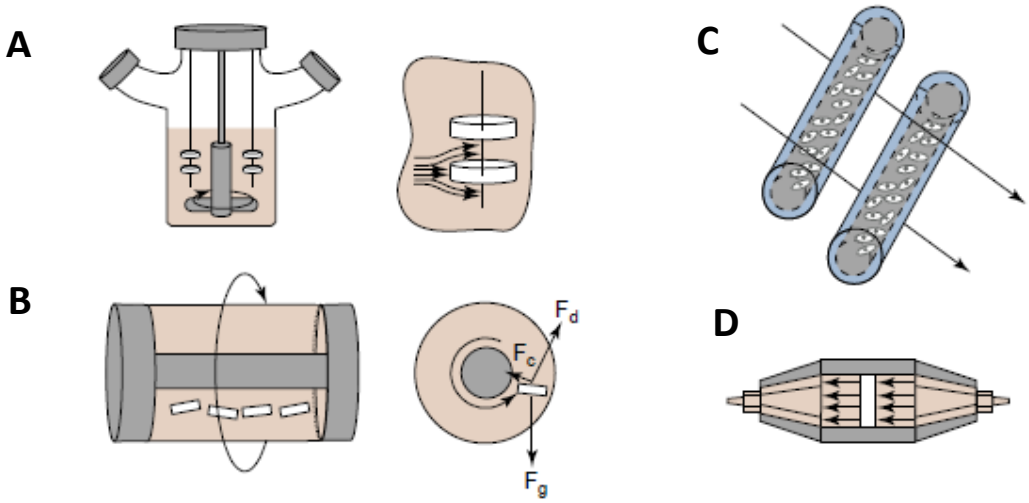

Figure 5. Bioreactors in tissue engineering. (A) Spinner flask bioreactors are usually used for cell seeding of scaffolds. Although mass-transfer is enhanced, generation turbulent could hinder tissue development. (B) Rotating-wall vessels allow dynamic culturing of scaffolds with low shear stress. Due to forces applied to the system are balanced the construct remains in free-fall state while operating. (C) Hollow-fiber bioreactors can enhance mass transfer especially for sensitive cell types such as hepatocytes. (D) Direct perfusion bioreactors allow medium to flow directly through the scaffold pore structure and can be used for both cell seeding and continuous culturing [184].

Among bioreactor types, perfusion systems are more effective for homogenous perfusion of culture medium throughout the scaffold. In addition to osteogenic markers, Alvarez-Barreto *et al.* showed that bioreactors with oscillatory flow regime can improve cell seeding into scaffolds with different architectures[124] while Janssen *et al.* reported homogenous cell growth and ability to O_2 consumption measurement in perfusion bioreactors[125]. Moreover, perfusion bioreactors are shown to upregulate osteoblastic markers and calcium deposition. In a study published by Bancroft *et al.,* rat marrow stromal cells seeded on titanium scaffolds were perfused at varying flow rates. The study suggested that, mineral matrix deposition was dramatically increased with increasing flow rates. Moreover, their data suggested that osteoblastic differentiation was accelerates as the flow rate increased[126]. In an another study, Holtorf *et al.* used rat BMSCs seeded on porous calcium phosphate ceramics suggested that osteoblastic differentiation of the cells were increased with the perfusion bioreactor[127]. Moreover, the same group showed that under flow perfusion rat BMSCs can differentiate into osteoblasts without osteogenic supplements[128]. Similarly, Gomes *et al.* and Bjerre *et al.* separately reported that flow perfusion enhances the calcium deposition and expressions of ALP, TGF-β1, VEGF, BMP-2, BSP, RUNX2, OPN and FGF-2 were increased of the scaffold seeded cells[129]–[131]. Wang *et al.,* reported a similar outcome in porous ceramic materials as the osteogenesis of bone marrow derived osteoblastic cells improved in perfusion bioreactor systems[132]. Such efforts allowed successful implantation of tissue generated in *in vitro* settings as Timmins *et al.* reported that human BMSCs in a perfusion bioreactor and obtained construct capable of inducing ectopic bone formation in nude mice[133]. Finally, Papadimitropoulos *et al.* reported a 3D bone organ model using a human-origin osteoblastic-osteoclastic-endothelial co-culture system to mimic bone turnover process under a perfusion bioreactor setup. The cells were perfusion-seeded into a ceramic scaffold and cultured under dynamic conditions. They showed that, after 3 weeks of culture, formation of bone-like tissue, blood vessels and osteoclasts after ectopic implantation to nude mice[134]. From enhanced mineralized matrix deposition to signal expression, bioreactors offer many advantages and results have been promising. Many studies with significant improvements compared to static systems have been proved that such systems could play a key role in bone tissue engineering applications.

2.4 Microfluidic devices for bone tissue engineering

Microfluidic environments provide an ideal setup for generation of functional 3D tissue models using various type of cells[23]. Similar to bioreactors, with the addition of shear stress factor, the generated tissue becomes an *in vivo*-like substitute which can be used in many studies including injury and disease models[135], drug safety and discovery[136], [137], organ specific models and multi-organ systems[138]. The main difference of microfluidics to bioreactors is that the microfluidic systems allow spatial control over fluids in microscale channels which increase physiological relevance of the system[139]. In other words, microfluidics can be used as microscale bioreactors with more control on environmental conditions. As a result, microfluidic bioreactors allow for the establishment of dynamic mechanisms that can be used to adjust the environment of the cells as an almost *in vivo* environment[21]. Over the years, such an advancement caused a broad focus on co-culture environments and cross-talks which are difficult to observe under any other setup[140]–[146]. Such efforts is hoped to achieve better tissue/organ models due the in depth understanding of cellular interactions. Using such systems several applications have been reported including lung, liver, heart, kidney and gut models (Fig. 6). Regarding the bone tissue, as mentioned before dynamic conditions are highly effective toward the regeneration and homeostasis of the tissue. Currently, a complete model of bone tissue which can perform bone remodeling processes is still challenging to generate[147]–[149].

Due to the complex and synchronous cellular interactions, many studies on bone cell response for mechanical stimulation are carried out in inadequate *in vitro* environments with single cell type. However, significant number of studies on osteogenesis in 3D setups have been reported. For instance, Middleton *et al*. reported one such study using 3D circular microchambers in a microfluidic device to study osteocyte formation and concluded that osteocytes can be cultured in 3D architecture and elucidated mechanotransduction mechanisms which is not possible with conventional techniques, however the setup contains sophisticated and time-consuming methods[150]. Another behavioral study was reported by Occhetta *et al.*, bone barrow-derived MSCs were cultured under continuous flow in a microfluidic device with a morphogen gradient, the authors were able to obtain 34-fold higher percentage of proliferating cell pellets compared to traditional culturing techniques in the period of a week[151].

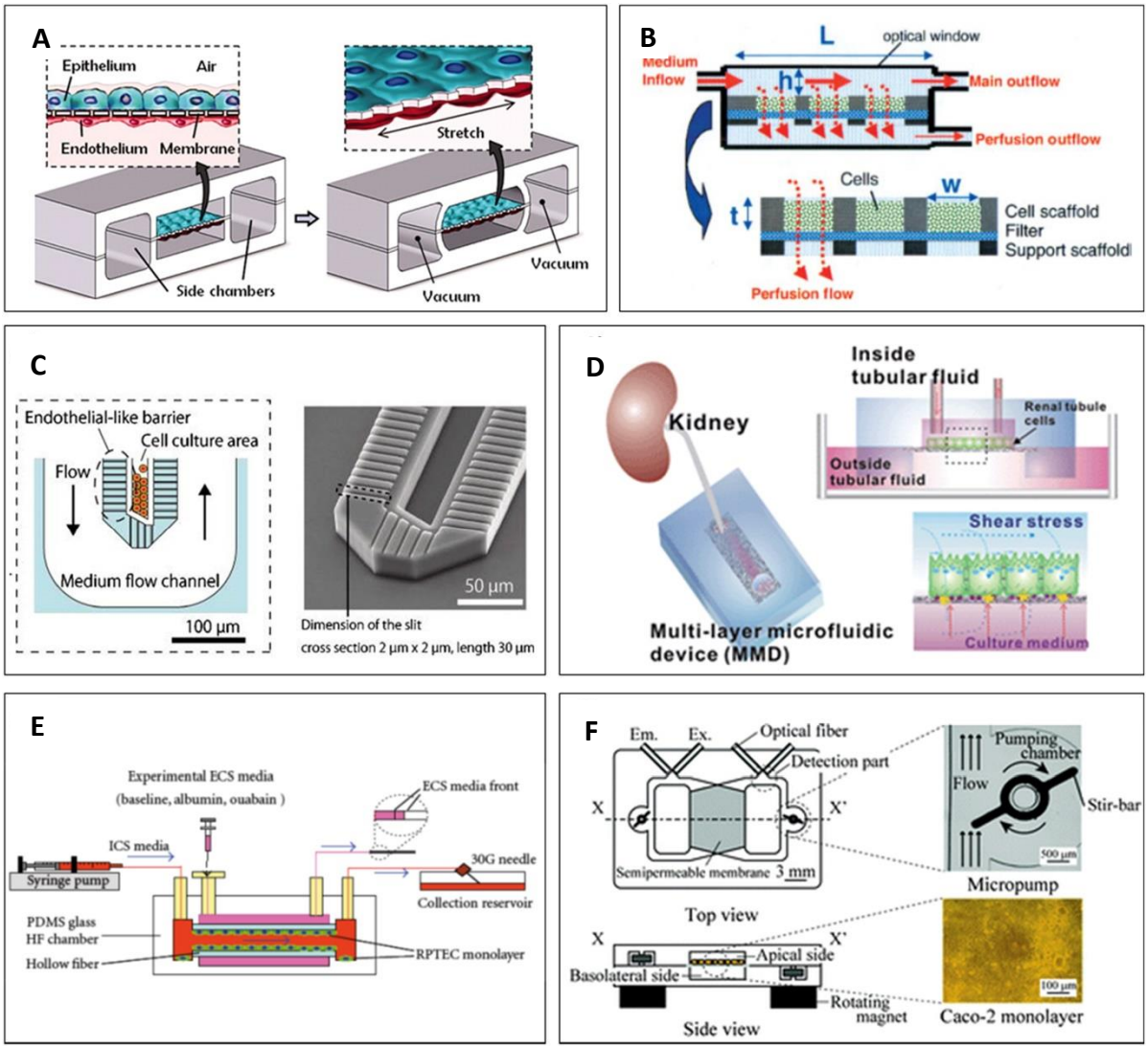

Figure 6. Organ-on-chip devices [185]. (A) Microfluidic lung-on-a-chip device that can mimic physiological breathing movements using vacuumed side chambers[186]. (B) Perfused 3D liver culture in a microfluidic setting[187]. (C) The microfluidic device mimicking structure of hepatic cord[188]. (D) The microfluidic kidney model with in vivo-like tubular environment[189]. (E) The microfluidic device with structure of renal tubule[190]. (F) The microfluidic gut model containing two separate compartment[191].

Another aspect that affects the cell behavior is the design of the microfluidic channels. The configuration and the dimension of the device may potentially provide misleading results. Wei *et al*. reported that reducing the channel width 4 times and the height 5 times increases osteocyte cell death due to the insufficient nutrient transport[152]. Moreover, dynamic studies have been

reported involving 3D scaffolds. For instance, Cartmell *et al*. used a 3D cellular construct and a stainless-steel perfusion block to investigate effects of perfusion rate on the cell-laden constructs. They reported that higher perfusion rate than 0.2 mL/min upregulates expression of Runx2, ALP and OCN and thereby enhancing osteoblastic activities[153]. After utilization of microfluidic devices took place in tissue engineering, Leclerc *et al*. used a 3D scaffold and polydimethylsiloxane (PDMS) based device to study osteoblastic cells in a PDMS based microfluidic device. The authors reported that cellular activity is highly dependent on flow rate induced stress, which is in range of 0.05 Pa to 1 μPa. Moreover, the design of the microfluidic channels has affected ALP activity and resulted 7.5 fold enhancement compared to conventional static conditions[17]. As the co-culturing of different cell types showed more promising results, the view of bone tissue engineering has shifted into investigation of cross-talks in *in vitro* studies. Correia *et al*. used a decellularized bone scaffold to co-culture human umbilical vein endothelial cells (HUVECs) and human MSCs under varying conditions to create a vascularized bone tissue. The study was performed under static conditions and proposed that this system can mimic endothelial-osteogenic precursor interactions *in vivo*[33]. The same group used the same strategy using a microfluidic device and achieved a human bone perivascular niche model on microfluidic device for metastatic colonization studies[154]. Bersini *et al*. used a similar methodology to determine extravasation process of breast cancer on bone metastasis. The authors achieved to provide a 3D quantitative data on extravasation and micrometastasis generation of breast cancer cells into the bone microenvironment for cancer biology and therapeutics[155]. Later, Park *et al*. compared adipose and bone marrow derived stem cells in a mechanically stimulated microfluidic device in terms of osteogenesis. The study suggests that mechanical stimulation upregulates integrin and osteogenic gene transcripts. In addition, the authors showed that bone marrow derived mesenchymal stem cells are more sensitive to the mechanical stimulation compared to adipose tissue derived stem cells[156]. As a different perspective, Torisawa *et al*. used a different approach to produce a bone-marrow on chip model to study haematopoiesis and hematologic diseases. Authors used an engineered bone marrow placed into mice model and later implemented the scaffold into a microfluidic device. Authors reported that after one week of culture, *in vivo*-like structures were seen in the microfluidic environment[157]. A similar study was conducted by Sieber and colleagues, using only primary human cells the authors were able to expand the culture time up to four weeks which is suggested that is a sufficient time span for drug testing[158]. Finally,

Jusoh *et al*. used a microfluidic device, which was incorporated with microvascular networks in hydroxyapatite extracellular matrix and endothelial/stromal cells to create a vascularized bone tissue microenvironment. The authors reported that angiogenesis was affected by mechanical stimuli and were able to generate enhanced angiogenic processes including sprout length, speed, number and lumen diameter[159]. Middleton *et al*. presented a microfluidic device containing different cell populations at physiologically relevant distances in the channels and exposed to different levels of shear stress to study osteocyte-osteoclast communication. The authors suggested that the device can be applicable for multicell population cross-talk studies[150]. George *et al*. developed a microfluidic system for both stimulating osteocytes and quantifying bone remodeling. The system provides a basic model for remodeling interaction using standard mechanotransduction tool which is isolated activity is quantified as a function of load[160].

Microfluidics provide the optimum conditions of the cells in a dynamic system and the ability of the cell signal molecules to interact more realistically and to make sudden interventions through the designed system. In addition, more than one type of analysis can be tried at the same time in microfluidic devices and can provide high-resolution *in situ* imaging. However, bone has been one of the most challenging tissues for *in vitro* modeling due to the lack of information about cross-talk and cellular interactions. Cellular responses, which are triggered by physical forces, are studied under mechanotransduction and one of the most important aspects of bone tissue generation is the presence of physical forces. Mechanical stimuli cause rearrangement of the cytoskeleton and cell attachment and consequently cell fate. Microfluidic systems can provide mechanical forces to the cells in several ways. These include shear stress and compressive forces, as the cells are encapsulated in the 3D setup, axial pressure can be applied to the system. In addition, the fluid flowing through the channels can induce a shear stress on cells, which is reported to be effective for bone cells. The cellular response to the applied force is dependent on the magnitude, frequency and the strain field[161]. Bone-microfluidic system can be adjusted further to improve the results by controlling such physical parameters[162]. Currently, many studies have been completed and such aspects of the field have started to be elucidated. Therefore, it is expected that the generated bone tissues in microfluidic setups soon will replace the conventional graft technology and provide a cheap, fast, low-risk and widely available solution for bone pathologies.

3 MATERIALS AND METHODS

3.1 Type of research

The research encompasses *in vitro* experimental studies.

3.2 Time and location of research

All of the research was conducted in September 2018 - March 2020 at Izmir Biomedicine and Genome Center.

3.3 The universe and sample of research

The universe in this study is the mouse bone tissue. Sample of the research include all bone cells and bone remodeling process.

3.4 Materials of research

Porous ß-TCP scaffolds were used for achieving 3D environment, ß-TCP powder was given by Bonegraft Co., Izmir. Bone marrow cells were isolated by sacrifice of C57/B6 mice by cervical dislocation at Izmir Biomedicine and Genome Center vivarium. All isolations were completed between September 2018-March 2020.

3.5 Variables of the research

Independent variables: cell culture medium, the ratio of fetal bovine serum and penicillin-streptomycin.

Dependent variables: Cell seeding density, porosity, volume and stiffness of the ß-TCP scaffolds.

3.6 Data collection methods

3.6.1 Porous β -TCP scaffold synthesis

For bioceramic scaffold synthesis existing protocols were modified[163]–[166]. Firstly, commercial β-TCP (Bonegraft Biomaterials Co. Izmir) in powder form was grinded using an agate mortar and pestle to achieve fine particles. Later, 10 % polyvinyl alcohol (PVA) (Sigma) w/v was prepared using a magnetic stirrer and mixed at a ratio of 1:1 w/w with the β-TCP powder to obtain ceramic slurry. Commercial polyurethane foam with various pore sizes was used as the template. Various geometries of foam were prepared with a laser cutter (Epilog MINI, Epilog, USA). The slurry was then impregnated to the foam using a pressure chamber (Fig. 7). After impregnation, the foams were dried at 60 °C overnight. Then, the dried specimens were sintered at 1100 °C for 2 hours. Finally, the specimens were autoclaved for sterilization.

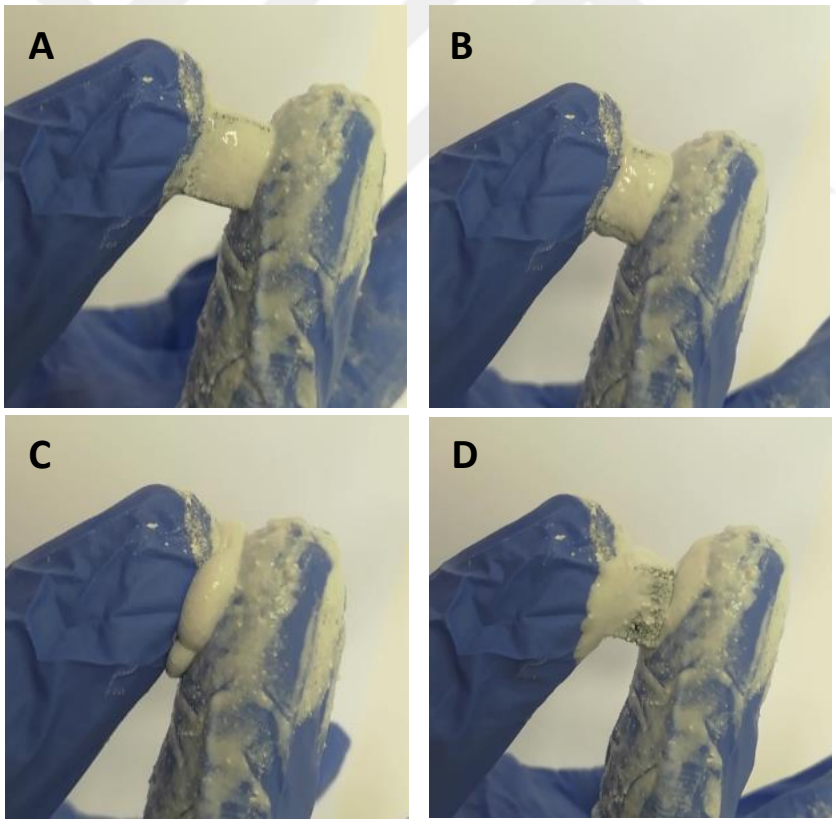

Figure 7. Ceramic slurry impregnated polymer foams. (A) Polymeric foam impregnated with ceramic slurry. (B-C) The impregnation can be evaluated by compressing the foam. (D) Ceramic slurry is removed as the pressure is applied from top and bottom sides.

3.6.2 Scaffold characterization

The particle size and distribution of the ß-TCP powder was measured before and after grinding (Mastersizer 3000, Malvern, UK).

Crystal structures of the ß-TCP powder before and after sintering procedure were determined by XRD analysis (Malvern Panalytical, UK) in powder form. The analyses were carried out at Izmir Kâtip Celebi University Central Laboratory Research Unit.

Compression strength measurements were acquired at Izmir Kâtip Celebi University Central Laboratory Research Unit in a universal testing machine (Shimadzu AG-IC, Japan). Sintered circular scaffolds were compressed uniaxially and compression strength and Young's modulus were calculated

The porous structure and interconnectivity of the scaffold were analyzed with SEM imaging (Zeiss, Germany). The specimens were coated with gold prior to imaging. Additionally, μCT analyses were carried out at Hacettepe University-HUNITEK (Bruker) to determine the porosities and inner structures of the scaffolds.

3.6.3 Microfluidic bioreactor fabrication

Microfluidic bioreactor was fabricated using rectangle polymethyl methacrylate sheets with dimensions 3 mm in height and 300 mm x 300 mm in cross-section. The bioreactor was designed in AutoCAD (Autodesk) and the sheets were cut using a laser cutter (Epilog MINI, Epilog, USA) (Fig. 8-9). Later, the bioreactor was sterilized using 70 % ethanol and UV curing.

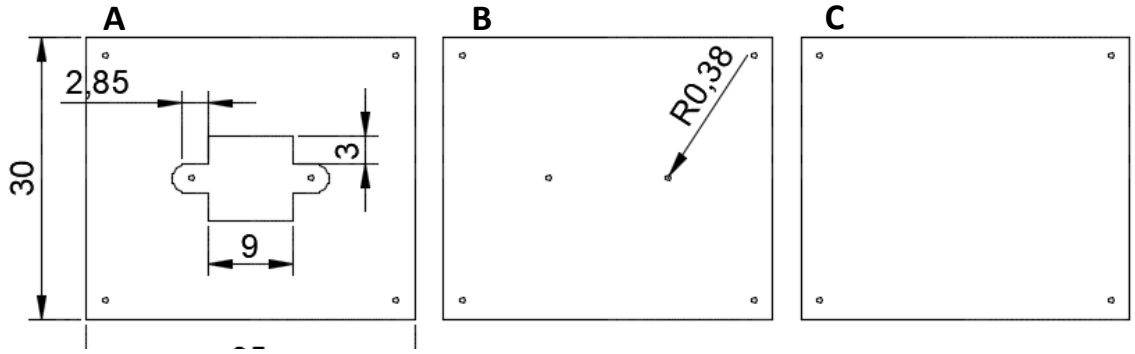

Figure 8. 2D drawing of the microfluidic bioreactor. (A) Channel layer that holds the ceramic scaffold, (B) top layer that tubings are attached to infuse medium, (C) bottom layer.

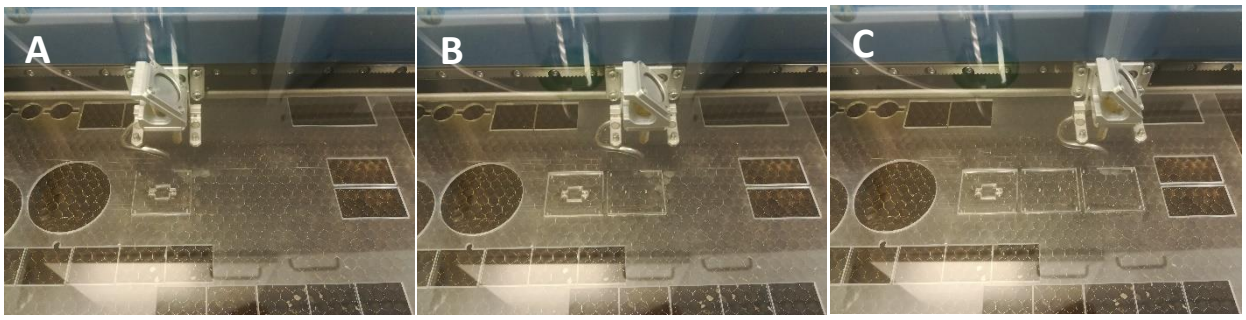

Figure 9. Laser prototyping of the microfluidic bioreactor. (A-C) Laser engraver followed a 2D CAD design and cut the PMMA sheets top to bottom.

After sterilization the bioreactor was assembled using leak-proof double-sided adhesive (3M). For dynamic culture syringe pump (Harvard) and silicon tubing (Tygon) were used. The cell-laden bioceramic scaffolds were placed in microfluidic bioreactor and dynamic cultures were initiated (Fig. 10).

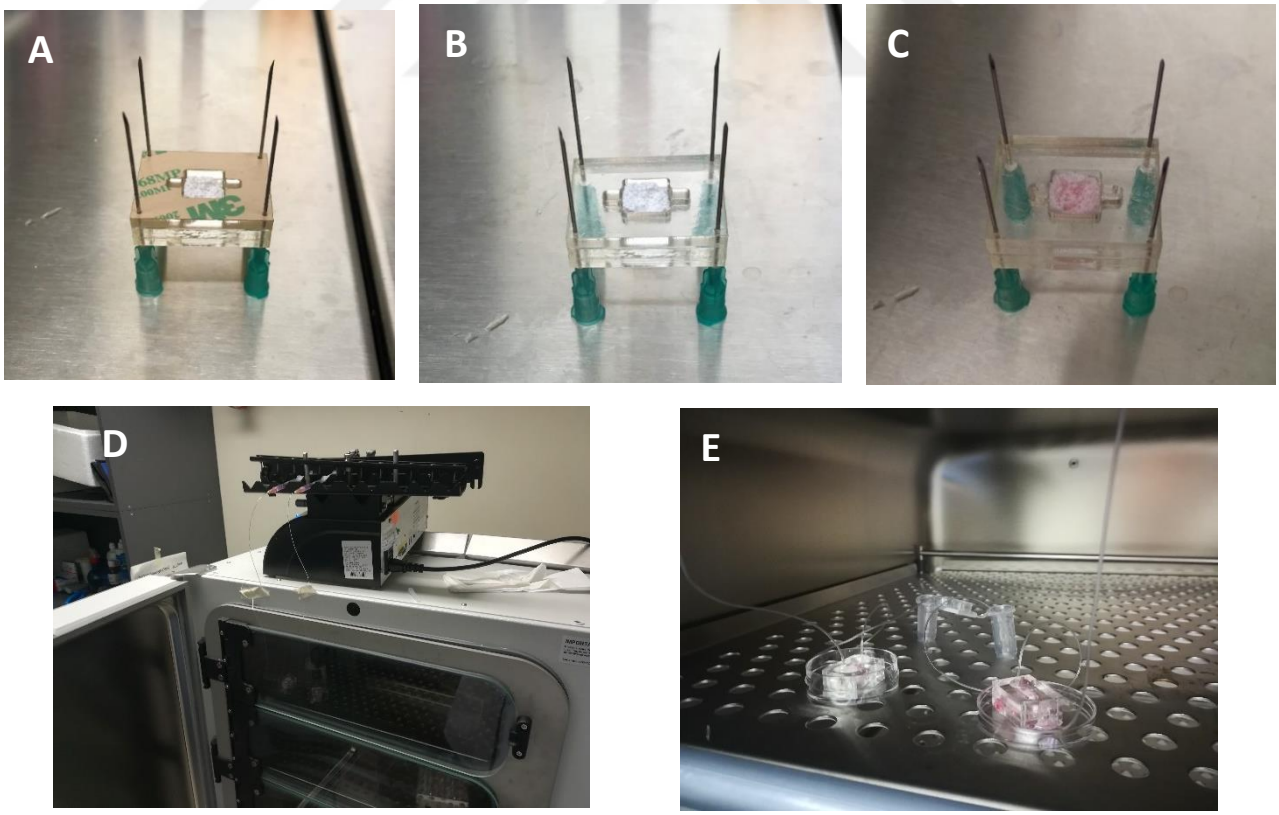

Figure 10. Dynamic culture experimental setup. (A-C) assembling procedure of the bioreactor, (D) syringe pump, (E) incubator setup.

3.6.4 In vitro cell culture studies

3.6.4.1 *Cell culture*

Mesenchymal stem cells and monocytes/macrophages were harvested and cultured from 4-8 weeks old Balb/c and C57BL/6 mice bone marrows with following procedure[167], [168].

Mice were euthanized by cervical dislocation and placed in a 70 % ethanol solution in a P100 cell culture dish (Orange Scientific) for 3 minutes. Further, all claws were dissected at the carpal joints and ankles and incisions were made around the connection between trunks and hindlimbs, forelimbs and trunks. Later, the skin was removed by pulling and soft tissues were carefully disassociated from tibias, femurs and humeri with micro dissecting scissors and surgical scalpel. After the dissection, tibias, humeri and femurs were cut from the joints and transferred onto sterile gauze. The bones were scrubbed to remove any soft tissue and transferred into a culture dish with 10 mL complete α-MEM (Pan Biotechnology, Germany) supplemented with 15 % FBS (Gibco) and 1 % penicillin-streptomycin (Thermo-Fisher) on ice. After all soft tissues were completely removed; the bones were washed twice with PBS. Later, the bones were transferred into a new culture dish with 10 mL complete α-MEM. The bones were held with forceps and the both ends were cut below the marrow cavity using scissors.

For mesenchymal stem cells, a 26-gauge needle attached to a 3 mL syringe is inserted to the marrow cavity and cells were flushed into the culture dish (Fig. 11). After flushing the cells were incubated at 37 °C and 5 % CO_2. The cells were cultured for 5 days. Later, the cells were washed twice with PBS and 2.5 mL of 0.25 % trypsin was added for digestion for 2 min. at 37 °C. Later, 7.5 mL of α-MEM supplemented with 15 % FBS was used to neutralize the trypsin and the plate was flushed with pipet-aid. The cells were then collected into a 15 mL centrifuge tube (Isolab) and centrifuged at 800 x g for 5 min. Later the cells were resuspended in a 75 cm^2 cell culture flask (SPL Lifesciences). The cells were passaged every 4-6 days at a split ratio of 1:3 (Fig. 12).

For monocyte/macrophages, a 26-gauge needle attached to a 10 mL syringe is inserted to the marrow cavity and cells were flushed with R5 medium, composed of RPMI supplemented with 5 % heat inactivated FBS, into a P100 culture dish and placed into an incubator at 37 °C

and 5 % CO_2. The next day, non-adherent cells were transferred to a 50 mL centrifuge tube and following culture conditions were set;

10 ml non-adherent bone marrow cells in R5 media

15 ml R5 medium

10 ng/ml M-CSF

The mix was cultured in an ultra-low attachment 6 well plate (Corning) as 4 ml/well and incubated for 7 days. On days 3 and 5, 2 ml of fresh R5 medium with 10 ng/ml M-CSF was added. On day 7, cells were centrifuged at 300 RCF for 5 minutes and washed with 1X PBS to obtain purified monocyte/macrophage cells.

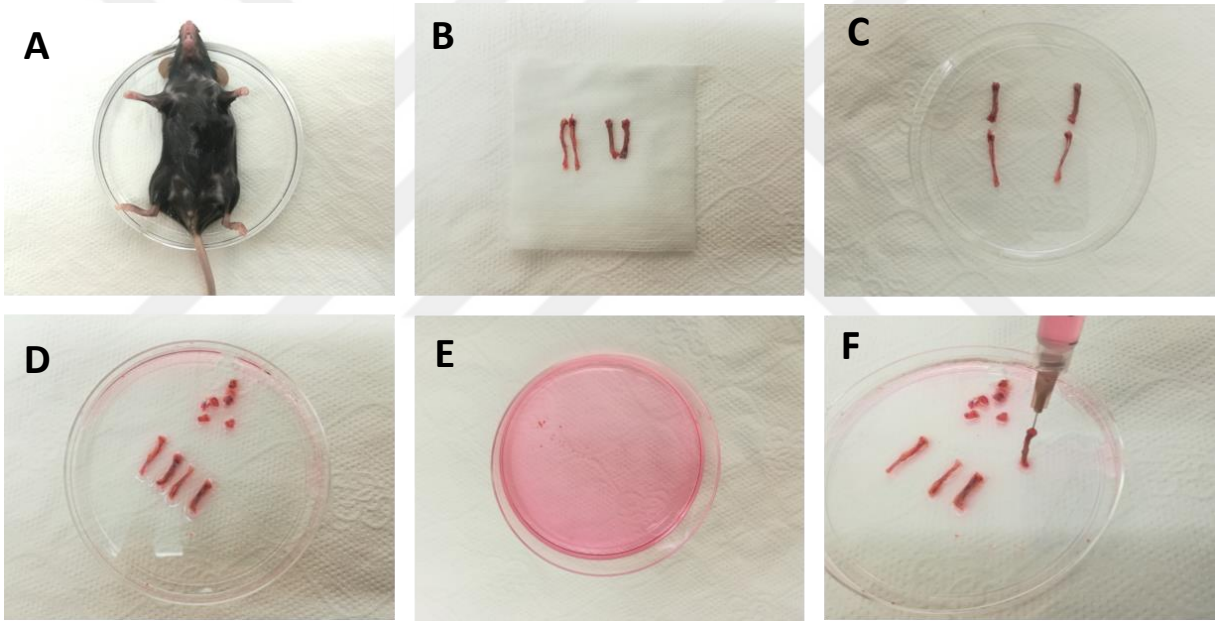

Figure 11. Cell isolation procedure. (A) Mice were sacrificed by cervical dislocation. (B-C) Femur and tibia bones were carefully dissected and all soft tissues were removed. (D) Marrow was exposed by cutting the bone at the ends. (E-F) Cells were flushed with a syringe filled with culture medium.

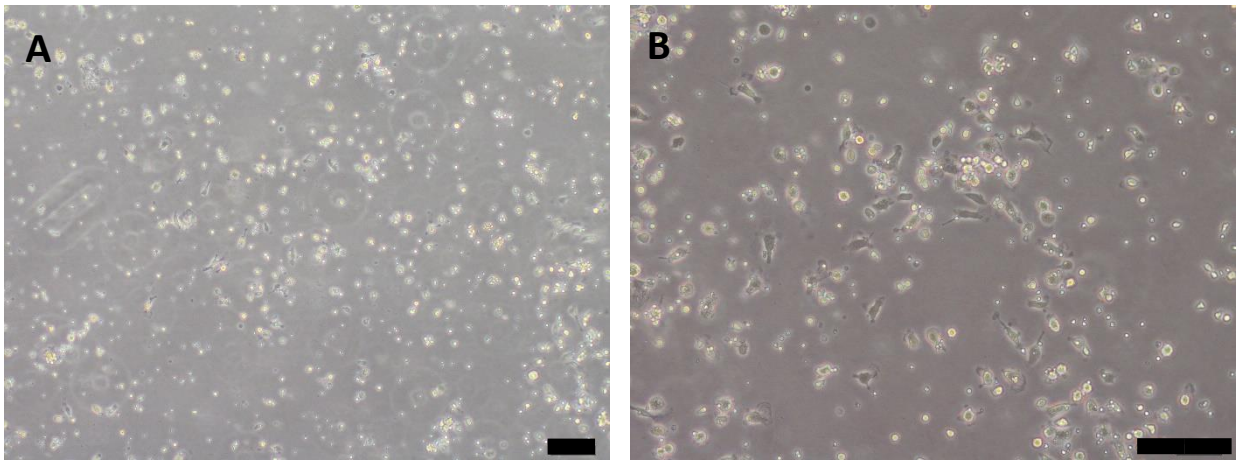

Figure 12. Isolated MSCs on day 5. (A-B) Light microscopy images show spindle shaped mesenchymal stem cells in the culture after 5 days of culture. Scale bar 100 µm.

3.6.4.2 *Cell seeding and proliferation studies*

Sintered ceramic scaffolds were autoclaved, seeded with 1 x 10^6 cells and incubated at 37 °C and 5 % CO_2 for 6 hours. Later, scaffolds were washed twice and 5 mg/ml MTT solution (Sigma) was mixed with phenol-free DMEM (Gibco). After 3 hours of incubation, scaffolds were observed for cellular proliferation under stereo microscope (Zeiss).

3.6.4.3 *Flow cytometry of isolated and differentiated cells*

Bone marrow cells were characterized with flow cytometry analysis (BD LSR Fortessa). After isolation of the cells red blood cell lysing buffer was added at a ratio of 5:1 and incubated for 2 min. at room temperature and centrifuged at 1200 rpm for 10 min. Later the cells were washed with FACS buffer containing 0.1 % sodium azide and 1 % bovine serum albumin and counted. The cells then distributed into tubes at a density of 1 x10^6 cell/tube. CD90 PE (Abcam - Cat no: ab24904) and CD105 FTIC (Biolegend - Cat no: 120405) markers were used for mesenchymal stem cells and for monocyte/macrophages CD14 PE (BD - Cat no: 553740), CD64 PE (BD - Cat no: 558455), CD45.2 APC-Cy7 (BD - Cat no: 560694), and F4/80 PE (BD - Cat no: 565410,) were used. Markers were diluted as manufacturer's recommendations and cells were incubated at 4 °C for 45 min. after staining. Then, the cells were washed twice with FACS buffer and fixed with 1 % PFA for 20 min. at room temperature. After another wash step, the cells were resuspended in 150 µl of FACS buffer before the analysis.

3.6.4.4 *Gene expression profiles of monolayer differentiated cells*

For qPCR analysis, TRIzol (Invitrogen) was used and manufacturer's protocol was followed (Macherey-Nagel, NucleoSpin RNA). First, the medium in the culture plate was aspirated and cells were washed by adding cold PBS. After the PBS was aspirated, TRIzol was added to the culture. After that, the cells were transferred to the 2 ml Eppendorf tubes and the cell lysate was thoroughly pipetted and vortexed to homogenize the cells and then incubated at room temperature for 5 min to allow the complete dissociation of nucleoprotein complexes. Later, chloroform with the ratio of 20 % per 1 ml of TRIzol was added and the tube was shaken vigorously for about 20 seconds and incubated at room temperature for 2-3 min. After the incubation step, the sample was centrifuged at 12000 g for 15 min at 4 °C to achieve phase separation. After centrifugation, the RNA layer in the aqueous phase was transferred to a new DNase, RNase-free Eppendorf and same volume of 70 % ethanol was added. The samples were mixed by pipetting up and down and incubated at room temperature for 10 min. Later, samples were washed, dried and eluted. Further, qPCR process was initiated using manufacturer's protocol (GoTaq® qPCR Master Mix). The primers used are given in Table 2.

Table 2. Primers used in gene expression studies

Gene	Forward (5' to 3')	Reverse (5' to 3')
ALP	CGAGCCGGAACAGACCCTC	GGCACAAAAGAGTTGGTAAGGC
Osteocalcin	GTCCAAGCAGGAGGGCAAT	AGATGCGTTTGTAGGCGGTC
Cathepsin K	TAGCCACGCTTCCTATCCGA	ACTGGGTGTCCAGCATTTCC

3.6.4.5 *Electron microscopy analysis of seeded ceramic scaffolds*

Cell-laden scaffolds were analyzed by scanning electron microscopy on days 7, 14 and 21 of dynamic culture. Fresh mouse bone was used as positive control. Sample preparation for SEM were performed by modifying published protocols[169], [170]. Briefly, scaffold samples were fixed with 2.5 % glutaraldehyde (Merck) in 0.1 M cacodylate buffer (Sigma) for 30 min. and were washed 4 times. Later, the samples were freeze-dried overnight in a lyophilizer (ThermoFisher). After drying process, the samples were coated 5 nm gold prior to imaging.

3.6.4.6 *Immunohistochemistry of cell seeded ceramic scaffolds*

Cells were fixed with 4 % PFA for 20 min prior to staining. Later, cells were stained with Phalloidin iFluor 488 (Abcam- Cat no: ab176753) and DAPI (Neofroxx-1322). Finally, samples were imaged with fluorescence microscope (Zeiss Olympus IX71).

3.7 Research Plan

Research plan of the thesis is given in the table below.

Table 3. Research plan of the thesis

	Sep. 2018 – Dec. 2018	**Jan. 2019 – Dec. 2019**	**Jan. 2020 – May 2020**
Literature Review	X	X	
Planning the Experiments	X	X	
Data Collection and Experiments		X	X
Evaluation of data		X	X
Thesis Writing			X

3.8 Evaluation of Data

For data evaluation, GraphPad Prism 7.1 was used to analyze results. $P < 0.05$ was accepted to be statistically significant.

3.9 Limitation of Research

Due to the global COVID-19 outbreak several experiments were hindered. Initially, it was anticipated to perform *in vivo* analysis after *in vitro* dynamic culture. However, due to the circumstances this was not possible. Therefore, *in vivo* analysis of cultured cell-seeded scaffolds was left out.

4 RESULTS

4.1 Characterization of the ß-TCP scaffold

4.1.1 Mechanical testing of fabricated ceramic scaffolds

Compression strength analysis results are given in Table 4. The mean compression strength of the scaffolds was found to be 1.72 MPa while mean Young's modulus was 140.38 MPa. The primary goal for stiffness was to be as close to natural bone. Changing the particle size of the powder and sintering has been significantly important for this aim. Consequently, we were able achieve the aim.

Table 4. Compression strength analysis

Compression Strength (MPa)	**Young's Modulus (MPa)**
1.56	128.02
1.82	152.06
1.67	140.52
1.75	135.62
1.82	145.67
1.72±0.11	140.38±9.22

4.1.2 SEM Imaging

The surface morphology and microstructure of the scaffolds without cells are presented in Figures 13-14. The scaffold exhibited a well interconnected structure with a microporous surface. The pore size was estimated in the range of 50 – 200 μm for macro pores and 1 to 10 μm for micro pores. Moreover, high magnification micrographs indicate the particle fusion is adequate.

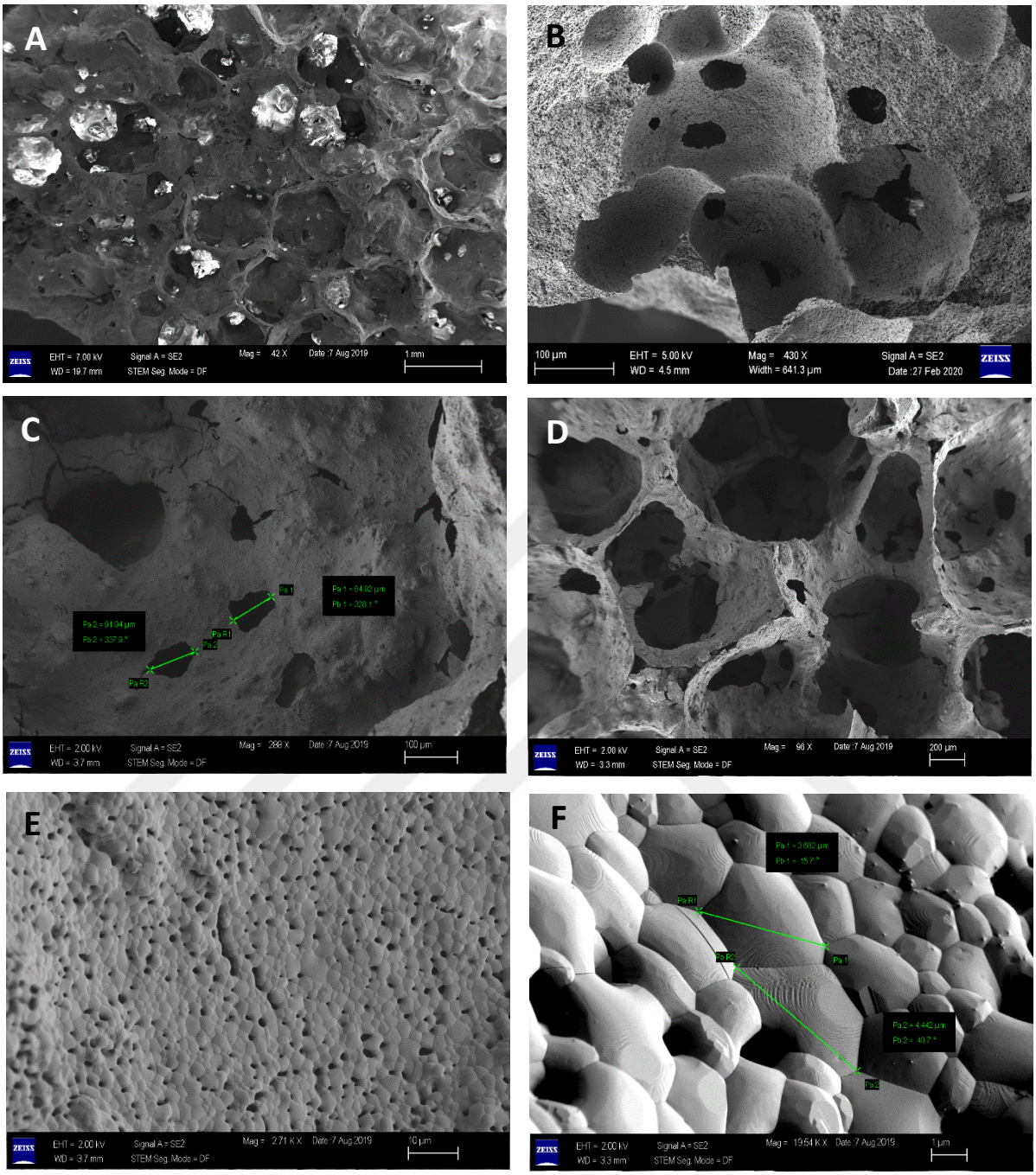

Figure 13. SEM analysis of scaffold without cells. (A-D) Interconnectivity of the scaffold can be observed with various macro and micro pores. (E-F) Surface structure shows uniform particle size distribution.

4.1.3 Particle Size Analysis

Particle size analyses before and after grinding of ß-TCP powder is shown in Figure 33. The Dv_{90} value for particle size before grinding was measured to be 180 µm while Dv_{50} was 52 µm. After grinding the Dv_{90} was decreased to 33 µm and Dv_{50} to 3.3 µm (Fig. 14).

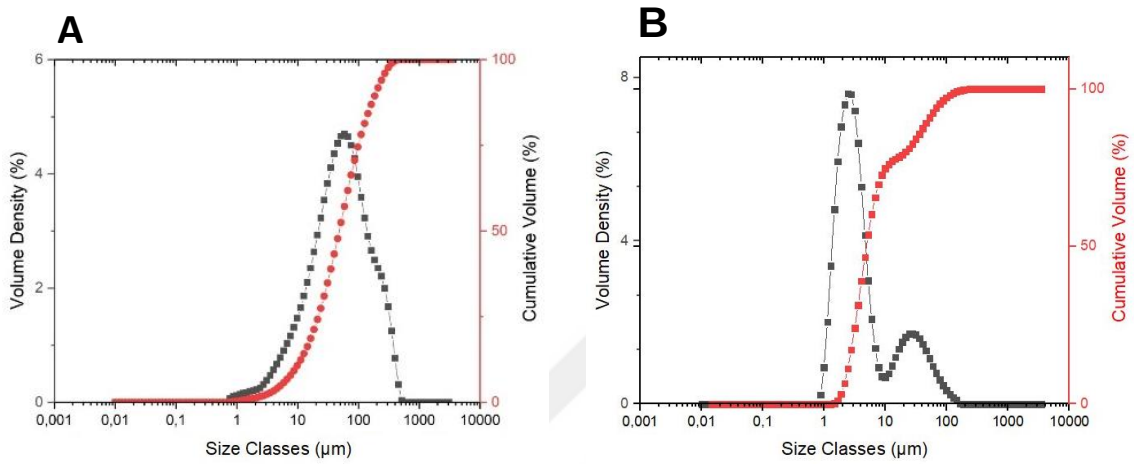

Figure 14. Particle size analysis of the ß-TCP powder before (A) and after (B) manual grinding.

4.1.4 µCT Analysis

µCT analysis of the scaffold is presented in Figure 15. In addition, calculated parameters for 4 specimens are given in Table 5. Both specimen 1 and 2 were manufactured in a rectangular shape with volumes 84 and 253 mm^3 respectively. Moreover, their porosity was measured to be 62.69 % and 73.68 % respectively. Specimen 3 and 4 were in cylindrical shape with volumes 46 and 211 mm^3 respectively. Further, their porosity was measured as 53.23 % and 57.5 % respectively. All specimens presented an interconnected structure with varying pore sizes and complex network.

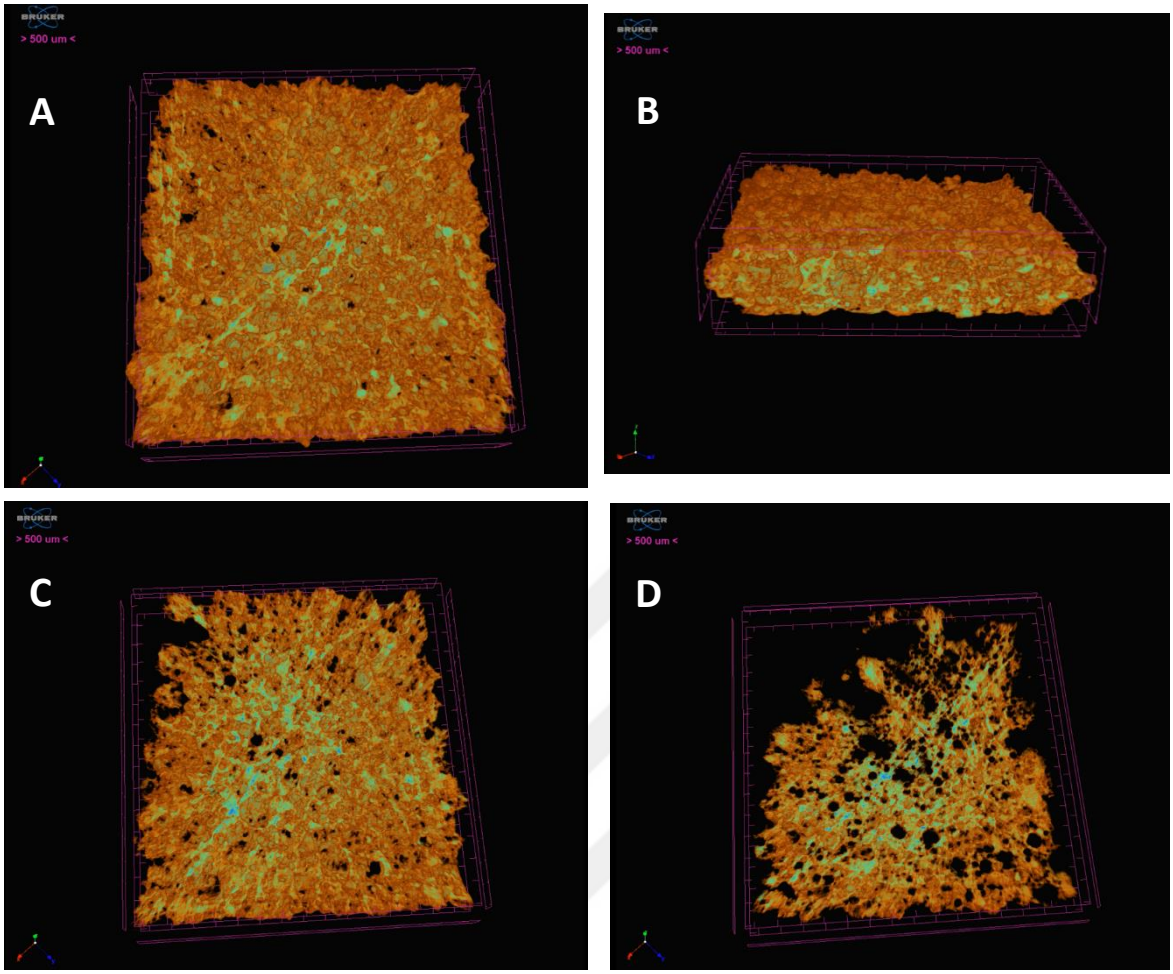

Figure 15. µCT analysis of the scaffold. (A-D) Flight simulator throughout the scaffold volume.

Table 5. μCT analysis results

Parameter	Specimen 1	Specimen 2	Specimen 3	Specimen 4
Dimensions(mm)	7.5x7.5x1.5	7.5x7.5x4.5	7.5xØ 2.5	7.5xØ 6
Volume (mm^3)	84	253	46	211
Number of closed pores	353	2609	764	8645
Volume of closed pores (mm^3)	0.01098	0.09026	0.068591	0.32972
Surface of closed pores(mm^2)	1.45308	11.02504	6.46133	42.01649
Closed porosity (%)	0.17256	0.17709	0.46376	0.3651
Volume of open pore space (mm^3)	10.70144	142.65143	16.82963	122.214
Open porosity (%)	62.6932	73.67739	53.2247	57.5044
Total volume of pore space (mm^3)	10.70144	142.74169	16.898221	122.5437
Total porosity (%)	62.75758	73.724	53.44163	57.6595
Euler number	-2341	-19670	-1545	-26973
Connectivity	3050	25083	2902	38593
Connectivity density ($1/mm^3$)	178.85681	129.54919	91.7754	181.5877

4.1.5 X-Ray Diffraction Analysis

Figure 16 shows the two samples prepared for the qualitative XRD patterns and analysed by the Rietvield method. Both samples indicated highly crystalline samples given by the narrow and sharp peaks with even baseline. Three main peaks were observed in both before and after sintering at 2Θ 27.781, 31.047 and 34.393, which are consistent with the main peaks of TCP (Figure 16). Additionally, XRD phase analysis confirmed that the samples are in ß phase (Figure 17).

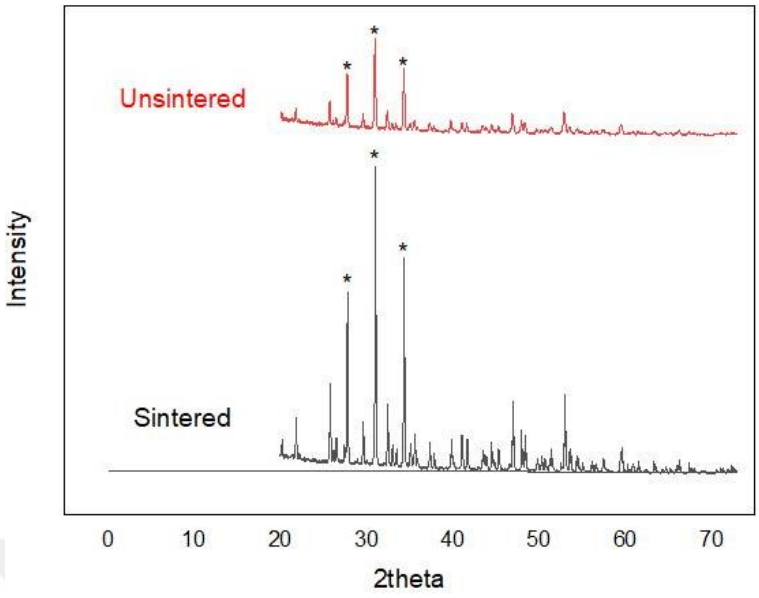

Figure 16. XRD pattern of the unsintered and sintered samples.

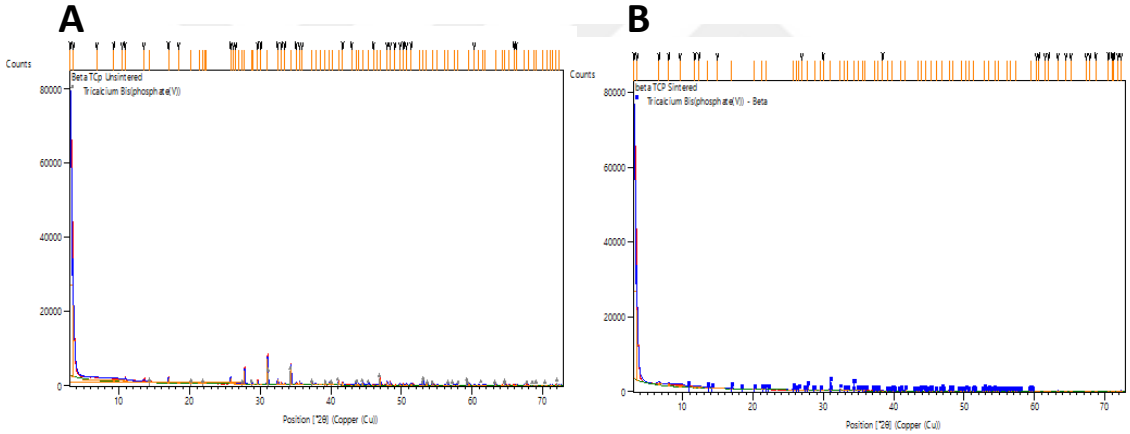

Figure 17. XRD phase analysis of the ß-TCP samples before (A) and after (B) sintering.

4.2 Expansion and differentiation of isolated cells

4.2.1 2D monolayer expansion culture of mBMMSCs

After 7 days of culture, isolated bone marrow cells exhibit various cell characteristics. Both spindle-shaped cells and colony-forming phenotypes are visible (Fig. 18).

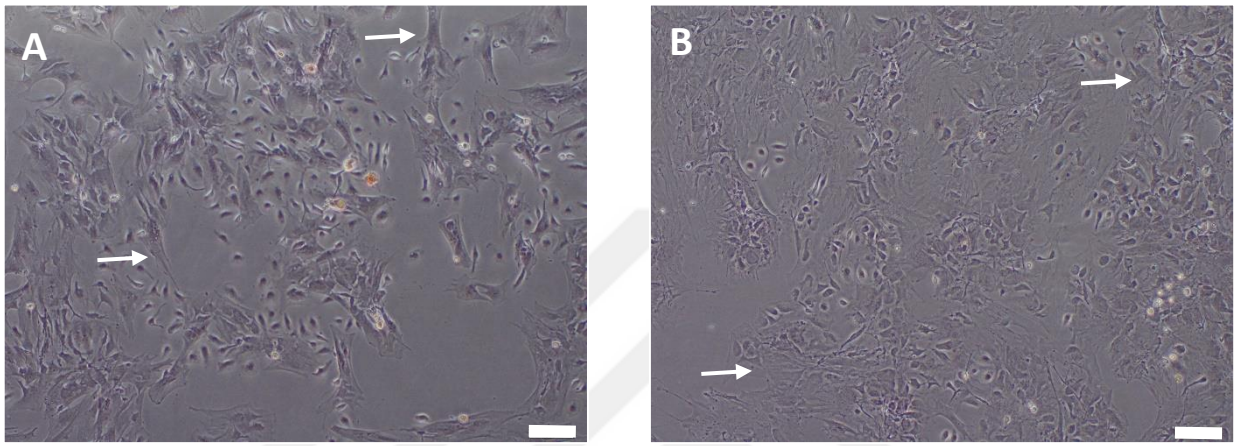

Figure 18. Day 7 of 2D culture scale bar, 50 µm. (A-B) Arrows indicating spindle shaped cells.

After 14 days of culture, spindle-shaped cells and colony-forming cells dominate the environment. We anticipated that the spindle-shaped cells are MSCs while colony-forming cells are monocyte/macrophages (Fig. 19).

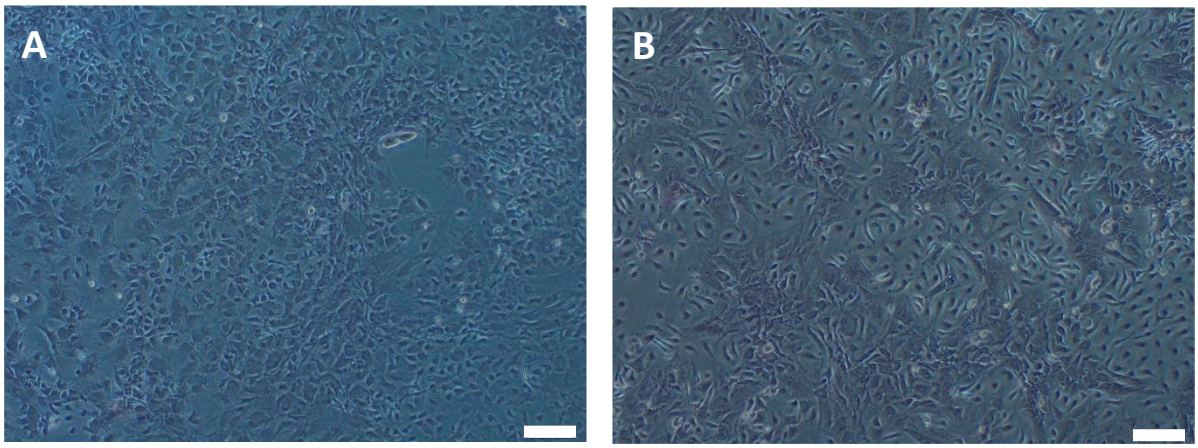

Figure 19. Day 14 of 2D culture scale bar, 50 µm. (A-B) After 14 days of culture, cells formed a close cell-cell interaction in the culture.

Moreover, alizarin red staining showed that the isolated cells can differentiate into osteoblasts and deposit calcium (Fig. 20). Consequently, showing that the culture contained MSCs.

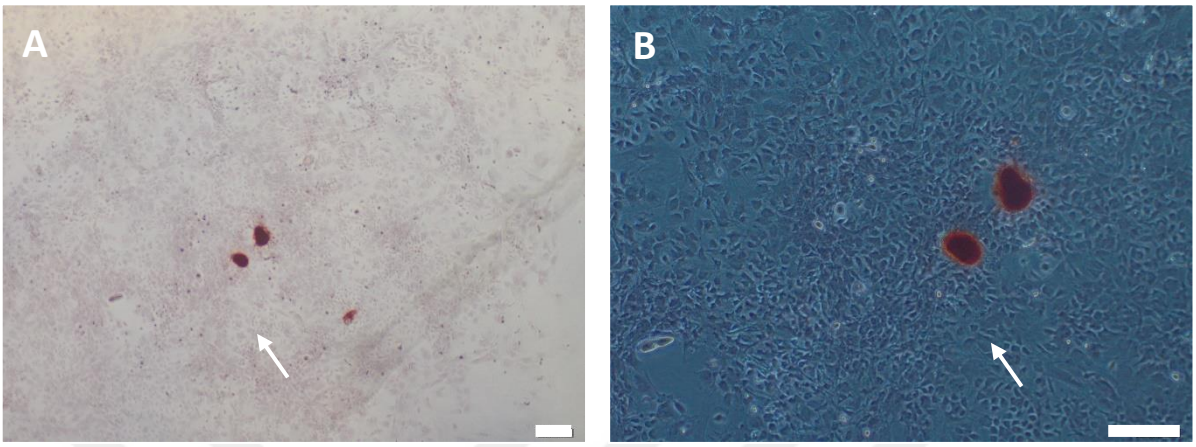

Figure 20. Alizarin Red staining scale bar, 50 µm. (A-B) After the culture calcium deposits were visible.

4.2.1.1 *Flow cytometry analysis*

Flow cytometry analysis before and after culturing are presented in Figures 21-22. Both mBMMSCs and monocyte/macrophage populations shows a dramatic increase after culturing.

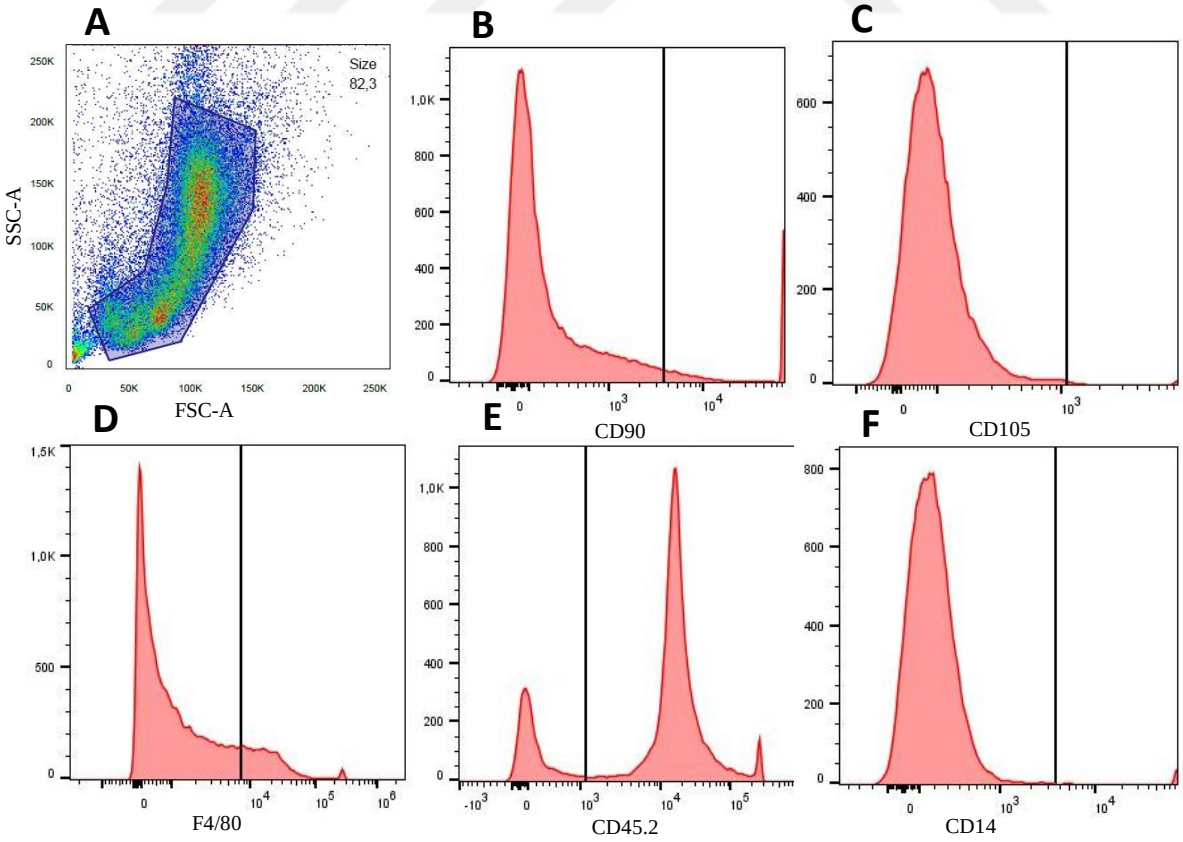

Figure 21. Flow analysis of freshly isolated mouse bone marrow cells. (A) total population zones. (B-C) Mesenchymal markers. (D-F) Monocyte/macrophage markers.

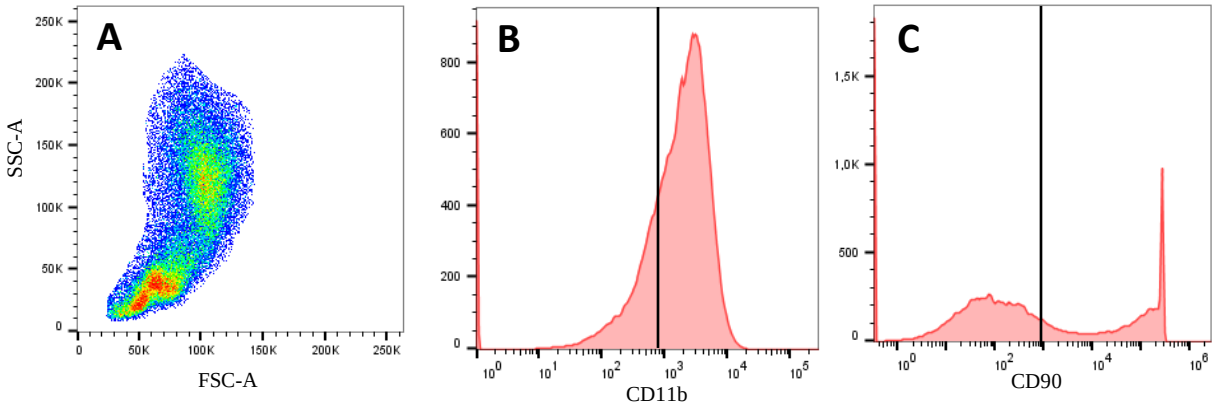

Figure 22. Flow analysis of cultured cells. (A) total population zones. (B) Monocyte/macrophage marker. (C) Mesenchymal stem cell marker.

4.2.1.2 *Gene expressions of differentiated cells*

PCR analysis results are presented in Figure 23. After 21 days of culture ALP, cathepsin K and osteocalcin shows a significant increase in fold change.

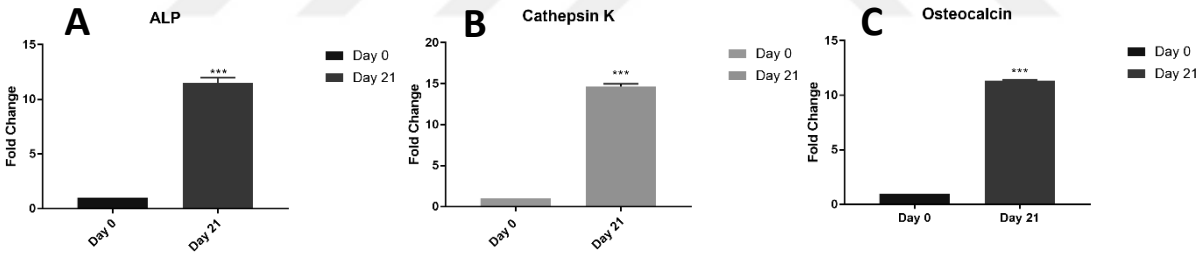

Figure 23. PCR analysis of cultured mBMMSCs and mMØ co-culture. (A) ALP protein levels are significantly higher indicating an osteogenic activity. (B) Increase in Cathepsin K indicates osteoclastic activity. (C) Osteocalcin levels shows a significant increase suggesting osteogenic activity is present.

4.2.2 3D culture

4.2.2.1 *SEM Imaging*

Figure 24 show SEM images used to evaluate attachment and proliferation of mBMMSCs and monocyte/macrophages on ß-TCP scaffolds. After 7 days of culture under dynamic conditions, cells were observed to be attached and formed junctions. Both macropores and micropores were observed to be invaded by cells. The adhered cells exhibited elongated morphology with several attachment sites. Moreover, cells did not appear rounded or clumped.

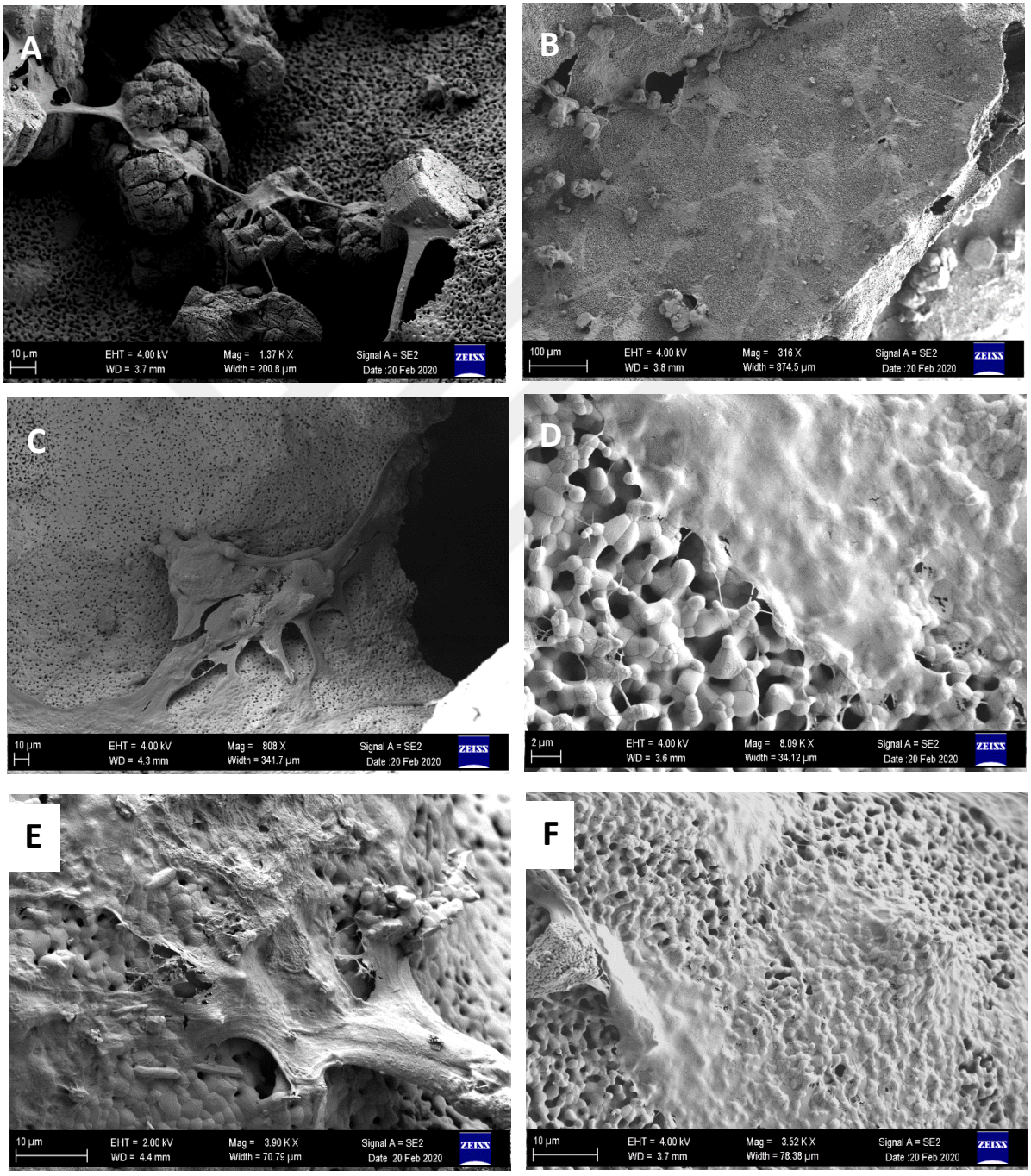

Figure 24. SEM analysis of cell seeded scaffold on day 7. (A-C) shows that the cells have started to form connections while attached to the scaffold. (D-F) shows that scaffold surface is highly suitable and favourable environment for cellular attachment.

Figures 25 show SEM images after 14 days of dynamic culture. SEM micrographs indicated an increased cell number on the scaffold. Moreover, cells were seen to form an increased amount of connections, covering large areas of the surface. Similar cellular morphology continued to be seen. Additionally, different sizes calcium phosphate crystals were observed.

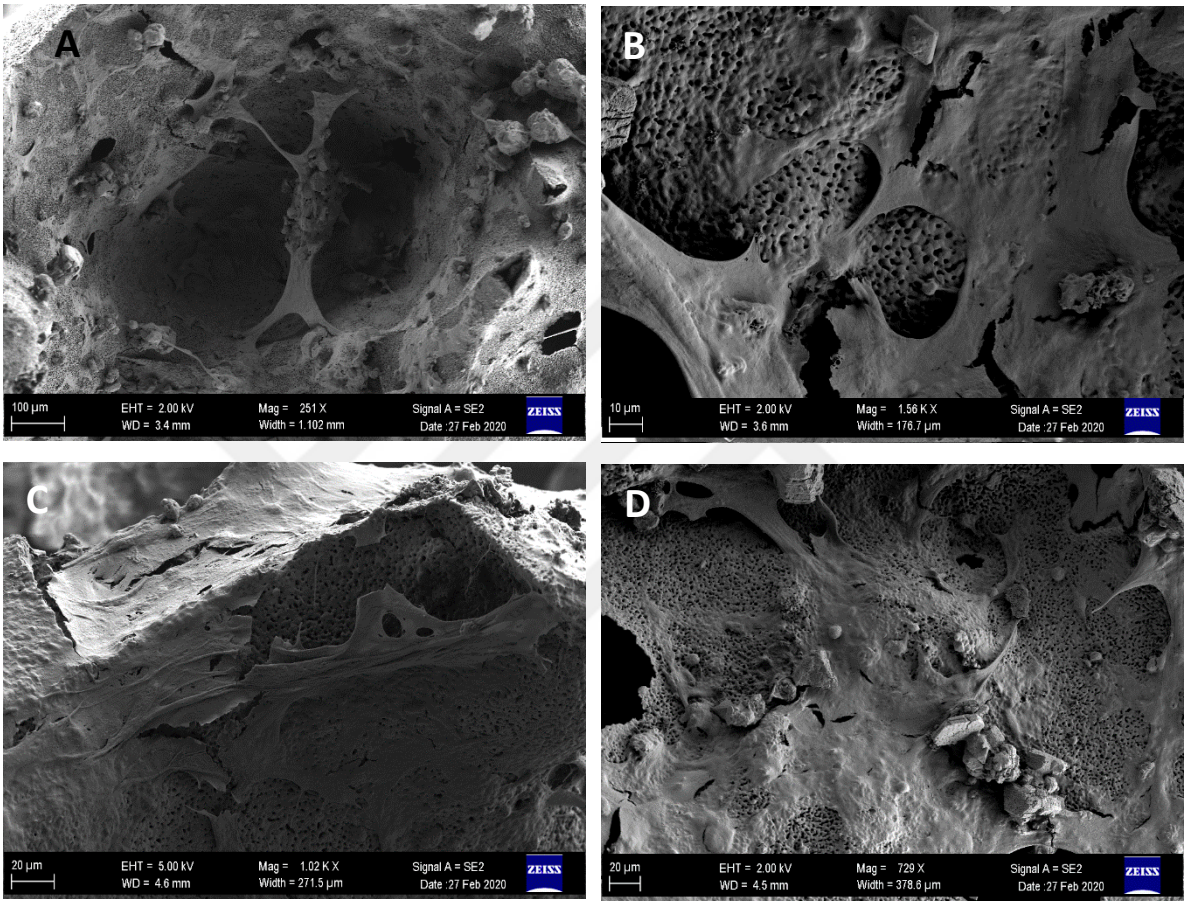

Figure 25. SEM analysis of cell seeded scaffold on day 14 of dynamic culture. (A) Macro pores of the scaffold are inhabited by cells. (B-D) Scaffold surface is partially covered with ECM.

Figure 26 shows SEM images of the seeded scaffolds after 21 days of dynamic culture. Micrographs indicated an increasing amount of ECM and cellular proliferation on the scaffold. Further, the scaffold surface was almost covered with ECM and cells appeared as small circles. Moreover, a web-like structure was seen in the layer underneath the scaffold surface.

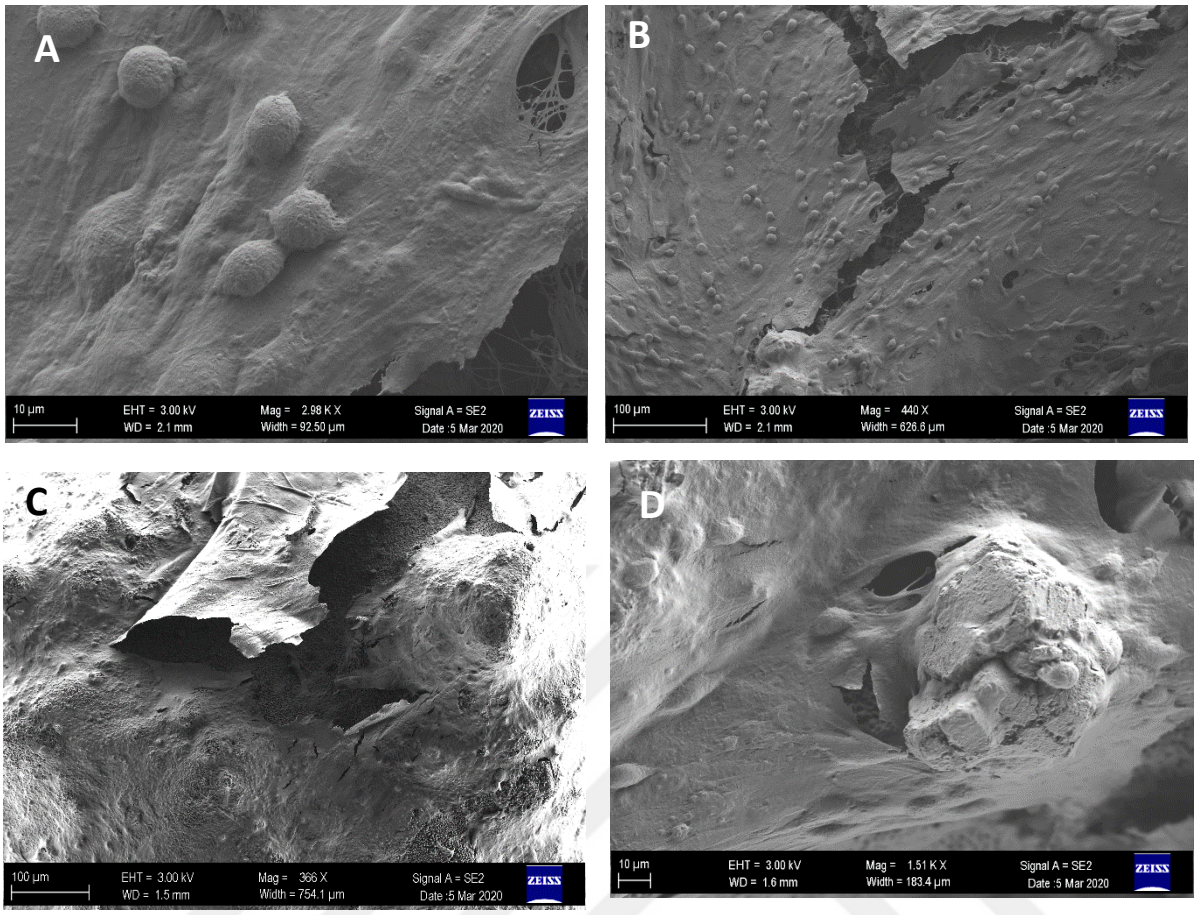

Figure 26. SEM analysis of cell seeded scaffold on day 21. (A-D) After 3 weeks of dynamic culture, scaffold surface was covered with ECM and cells were distinguishable. Inner sections of the structure were reached by cells and a web-like formation was seen.

Figure 27 show SEM images of freshly isolated mouse femur heads as positive control. The micrographs showed that a dense ECM with circular cells attached in the structure. Additionally, a web-like structure was seen to cover the surface of the femur head. Further, several blood cells were seen.

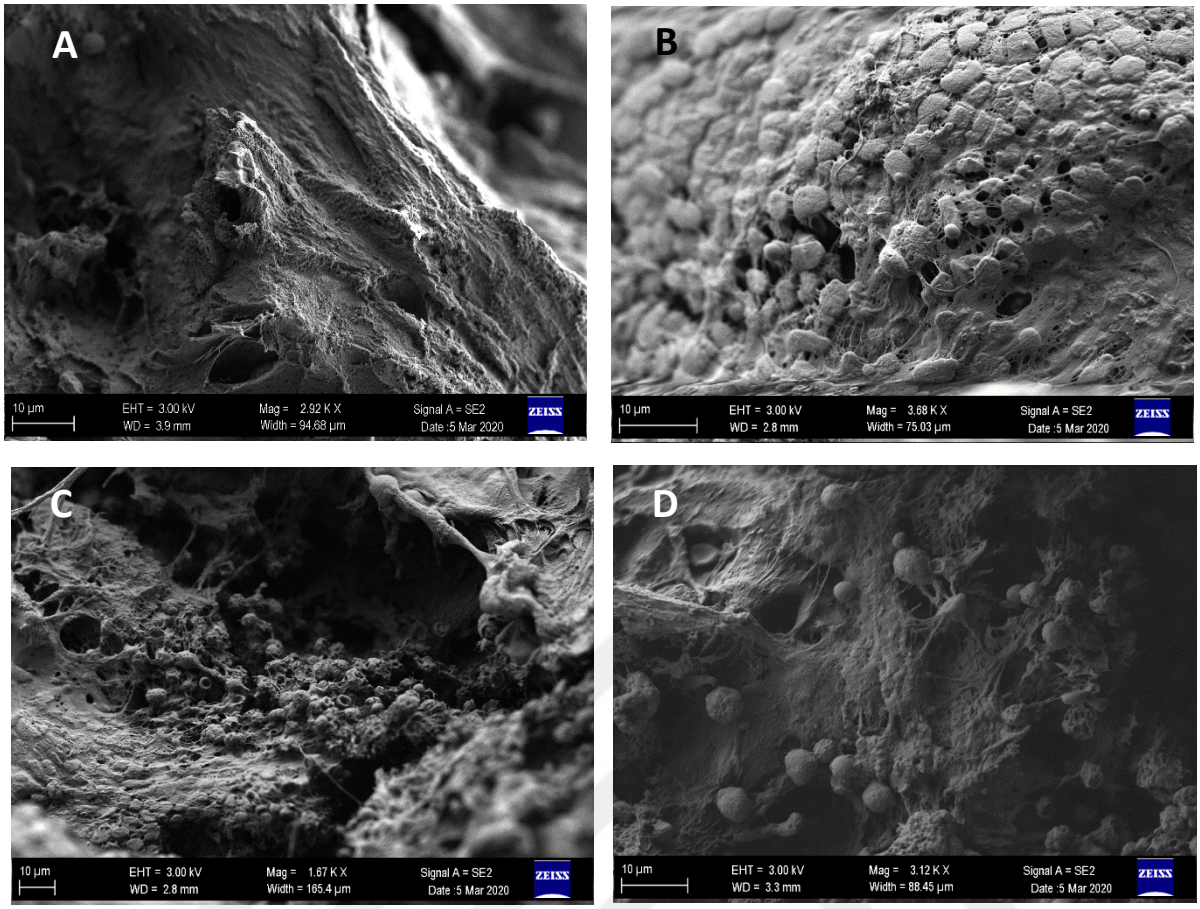

Figure 27. SEM analysis of freshly isolated mouse femur head. (A-C) a dense ECM structure can be seen on the surface of the femur tissue. (D-F) Cells in ECM are distinguishable at varying densities.

4.2.2.2 *Distribution of seeded cells*

MTT was used to visualize the cell-seeding efficiency into scaffolds. Purple color indicates formation of formazan (Fig. 28). Consequently, cell-seeding efficiency can be evaluated.

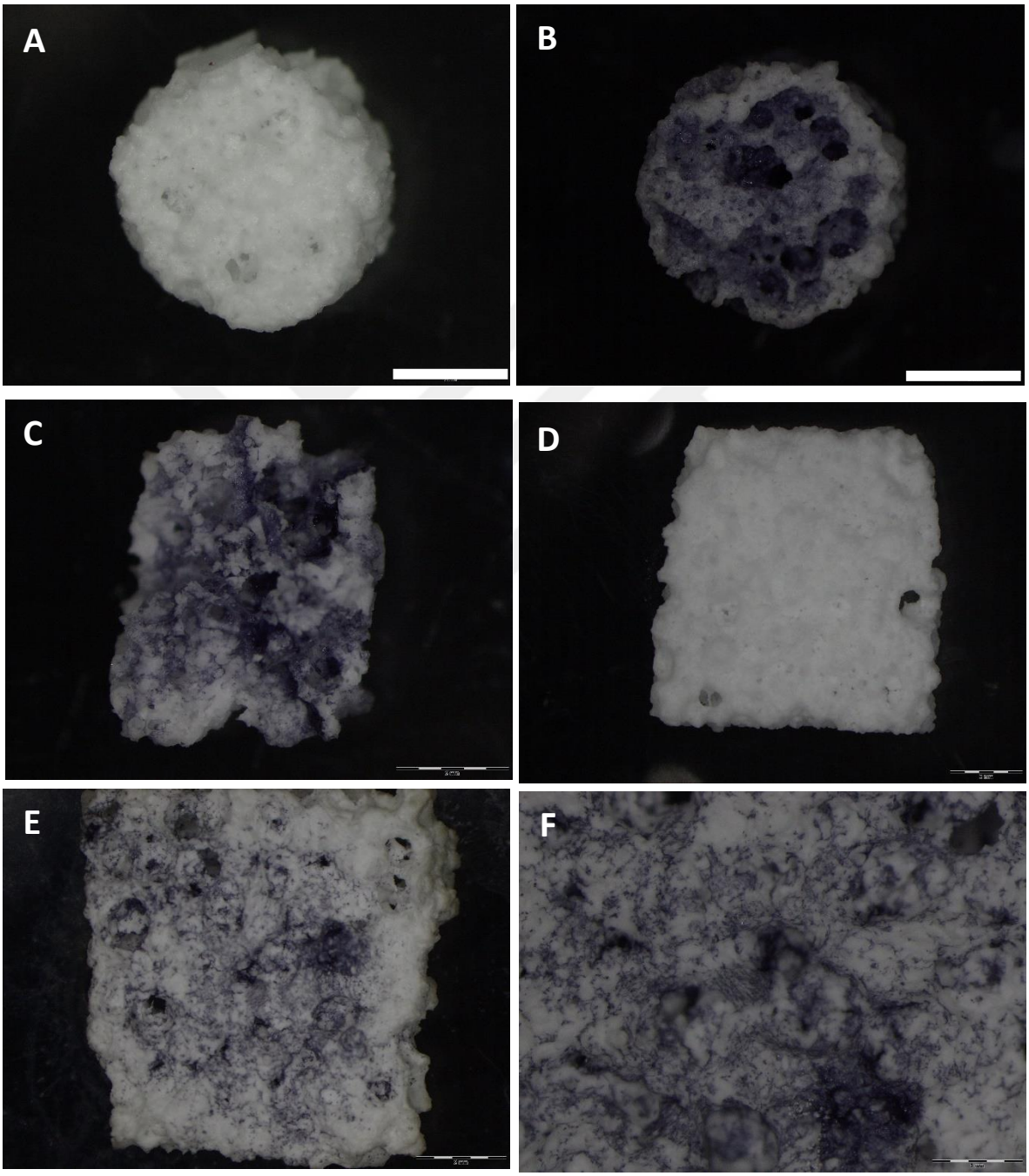

Figure 28. MTT stained scaffolds scale bar, 2 mm. (A-C) Unstained and stained top views of cylindrical scaffolds, (D-F) Unstained and stained top views of square scaffolds.

4.2.2.3 *Immunohistochemistry*

Immunohistochemical analysis of unseeded scaffolds are presented in Figures 29-30. Results indicate a slight autofluorescence before staining with Phalloidin iFluor 488 and DAPI. After staining and repeated washing steps same autofluorescence with unseeded stained scaffolds were not observed for both Phalloidin iFluor 488 and DAPI.

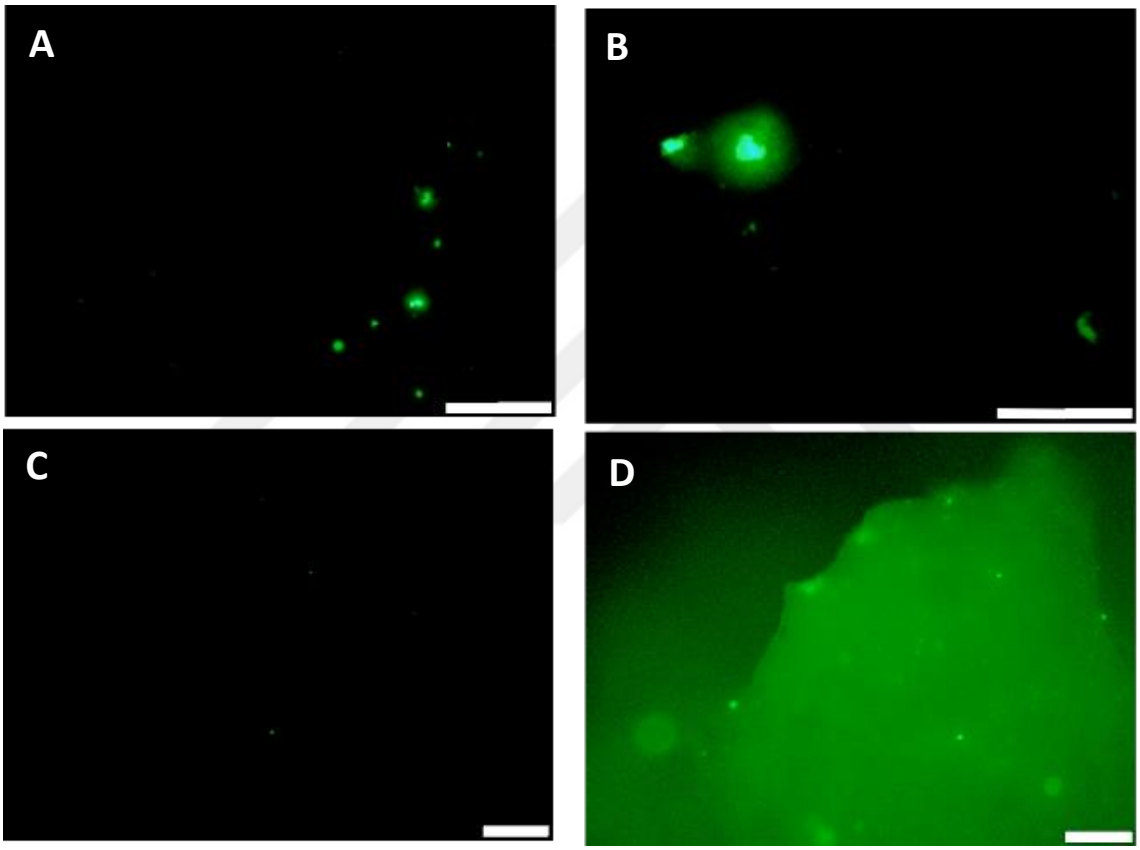

Figure 29. Autofluorescence measurement of unstained (A-B) and stained (C-D) unseeded scaffolds scale bar, 100 μm.

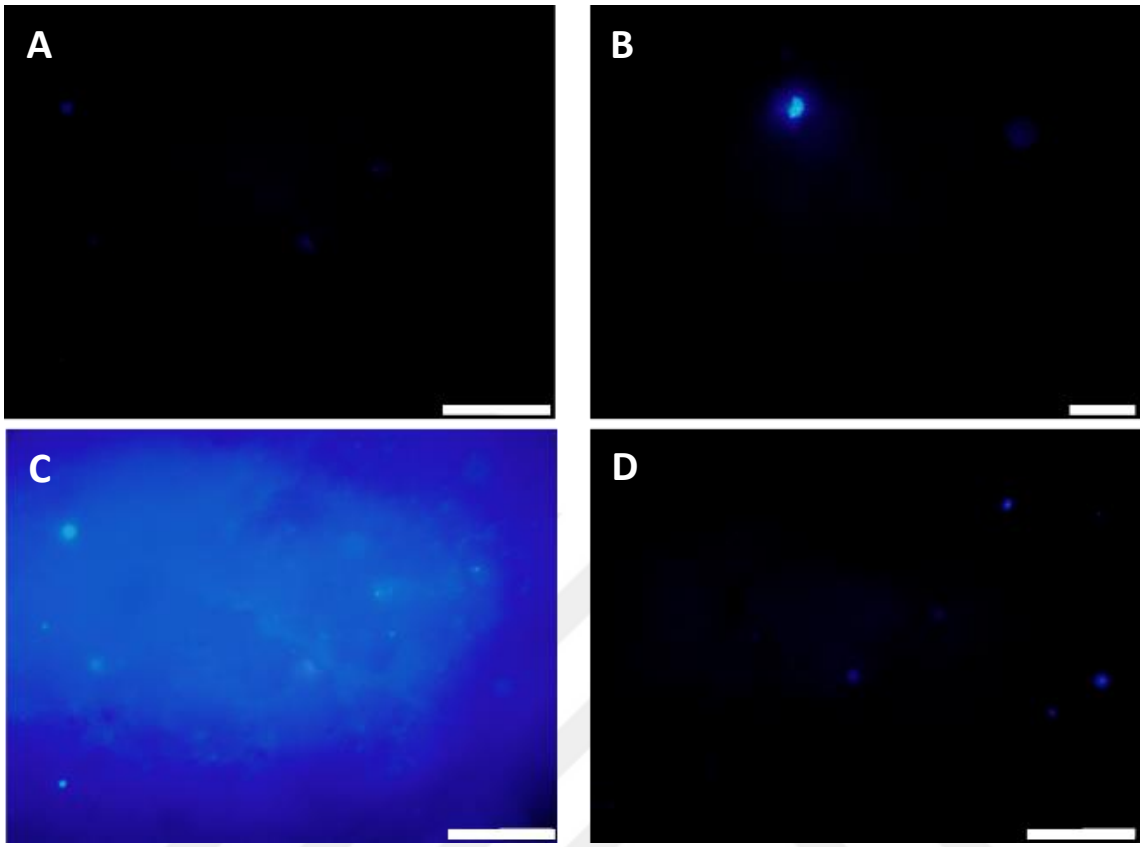

Figure 30. Autofluorescence measurement of unstained (A-B) and stained (C-D) unseeded scaffolds scale bar, 100 µm.

After autofluorescence measurement, mBMMSCs and mMØ were seeded on scaffolds for immunohistochemical analysis (Figure 31). DAPI-Phalloidin iFluor 488 staining showed clear images without any autofluorescence. Cell nucleus and actin filaments are clearly observable, on a dark appearing scaffold.

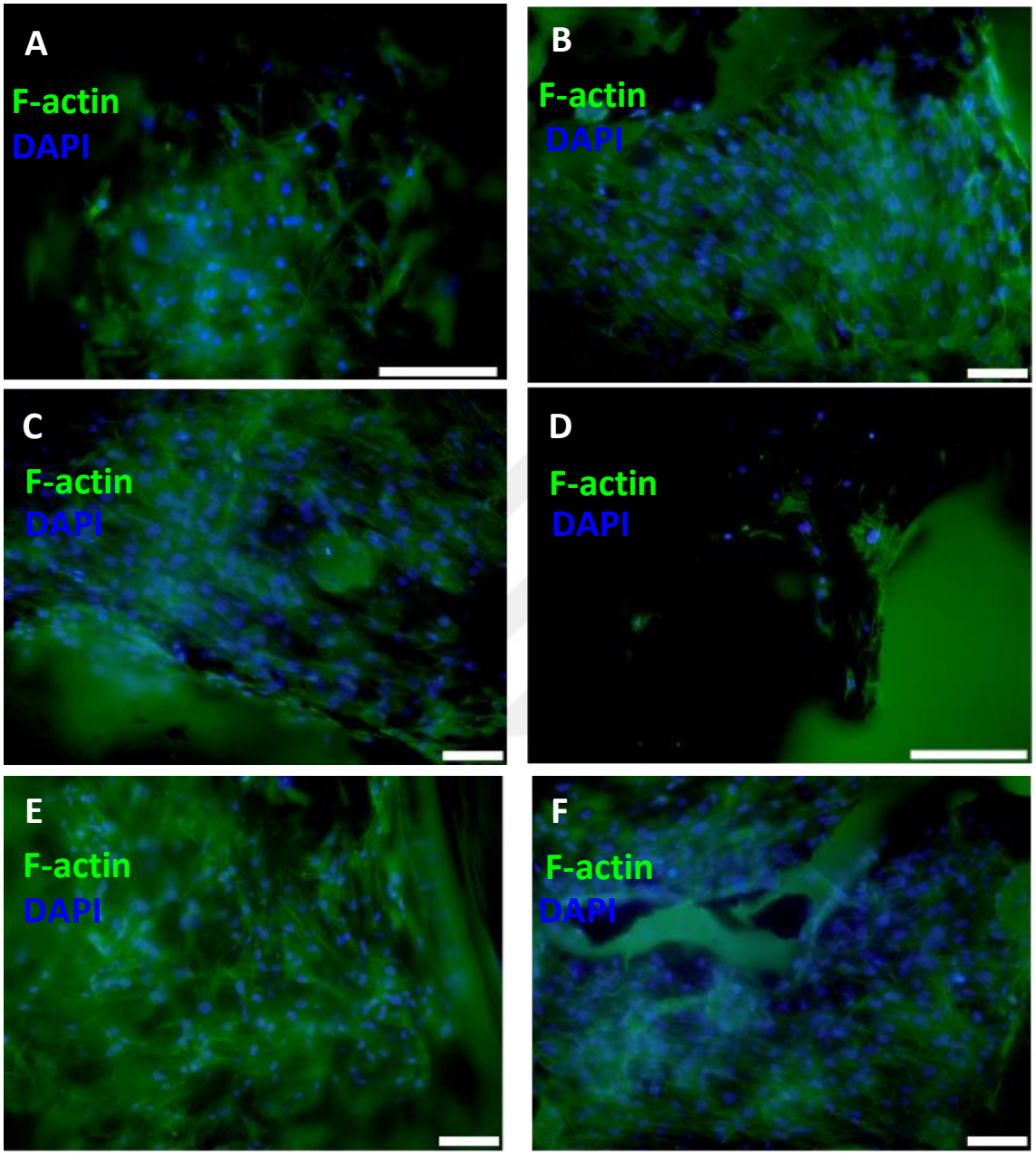

Figure 31. DAPI-Phalloidin iFluor 488 stained cell seeded scaffolds scale bar,100 μm. (A-C) Fluorescent microscopy showed that the scaffold surface and (D-F) inner layers were inhabited by cells.

5 DISCUSSION

In the first step of this study we attempted to manufacture a ß-TCP scaffold that can provide basic inorganic bone microenvironment. Moreover, we tried to tackle some of the problems that are often faced upon using ceramics for tissue engineering applications such as imaging difficulties. This attempt proved that it is possible to manufacture a porous ß-TCP scaffold that matches mechanical properties of the natural bone with a simple and robust protocol while suitable for dynamic culturing conditions (Fig. 1). Being a non-conductive and opaque, ceramics pose a challenge for usage in *in vitro* models. Consequently, these difficulties hinder reproducibility of the system. Moreover, manufacturing a tailored scaffold requires many considerations for optimum results. These include, imitation of natural ECM, biocompatibility, suitable surface properties, adequate mechanical properties, interconnectivity, suitable porosity, osteoconductivity and osteoinductivity [31], [171]–[173]. In addition to these properties, another important aspect for us was to be able to obtain fluorescence images from the structure after the culturing period. In order to achieve this, we decided to manufacture the scaffolds as thin as possible, allowing stained specimens to emit light. Moreover, while reducing the thickness we tried to keep mechanical properties as close to bone as possible. By using a foam replication method with a pressure chamber, we were able to fill the polymeric replica densely without losing porosity and strength (Fig. 7 & Table 4). In fact, by changing the pore size of the replica, we were able to manufacture different porosity percentages (Table 5). In addition, XRD analysis indicated that the structure is mainly ß-TCP before and after sintering (Fig. 17). Further, the µCT analysis confirmed an interconnected structure resembling the native bone environment (Fig. 15). Moreover, using a polymeric sponge allowed manufacturing various shapes and sizes that can be tailored for any bioreactor setup. After reaching to less than 2 mm, florescence images significantly improved (Fig. 31). Another aspect in the manufacturing process was the surface shape. The importance of this step stemmed from the necessity of providing an easy anchorage site for cells. Also, easy ECM formation between cells using micro pores on the surface. Due to the seeding of the cells was from top to bottom, this step has been of importance to form a dense ECM network all over the scaffold volume. In order to achieve this, we decided to lower the particle size of the ß-TCP to Dv_{50} of less than 10 µm by a grinding process. The initial particle size was Dv_{50} of 52 µm, at the end of grinding process we achieved Dv_{50} of 3.3 µm (Fig. 14). This process not only reduced

the particle size significantly, but also allowed uniform particle shape, which was crucial to form a ceramic network (Fig. 13). As Saiz *et al*. reported, smaller grain size not only increases the mechanical strength but also provides a more favorable anchorage site for attachment and proliferation of cells [174]. Supporting the article, SEM micrographs showed that the network contained micro pores that cells can reach from the surface to deeper sections of the scaffold (Fig. 13). Moreover, after 21 days of culture the scaffold surface has been covered with ECM. In addition, macro pores allowed cellular transport during cell seeding and allowed cells to invade deeper sections (Fig. 26). Therefore, the cells on higher levels were able to form junctions and secrete ECM with the cells on lower levels with ease. Further, MTT assay was used to visualize the cellular proliferation on scaffold. After 6 hours of culture, the formazan formed can confirm that majority of scaffold sites were invaded by cells (Fig. 28).

Another important aspect was the cell source for the model. Although, many single cell type cultures are developed, most are for the intention of studying cell morphology[175], differentiation patterns[176] or molecular pathways[177] for regenerative medicine and tissue engineering applications. However, as mentioned before, signals traded between osteoblasts and osteoclasts are crucial for bone remodeling process and thus, an *in vitro* system aiming to mimic this process requires simultaneous presence of these cross-talk processes and molecular mechanisms. For osteoblast cells, although different cell sources are used, isolation site can affect the final cellular feature. Among these sources, BMMSCs provide several advantages including easy cell isolation, high proliferative activity and osteogenic differentiation[178]. Osteoclast cells on the other hand, can be differentiated from BM monocytes which can differ from the ones that are harvested from peripheral blood[179]. Isolated monocytes are usually differentiated using M-CSF and RANKL factors which promote the fusion of monocytes and are essential for commitment toward osteoclastic differentiation[180]. Therefore, using only BM is sufficient for both MSCs and monocytes required to create a basic bone organ model that can perform bone remodeling using standard techniques. Additionally, using the tailored scaffold, these cells can retain their morphology and phenotype to accomplish their functions. Finally, a dynamic bioreactor the setup can allow engineering physiological, biomechanical and biochemical microenvironment all together. Therefore, we decided to use primary mBM cells as our cell source.

A co-culture model requires selection of suitable parameters such as culture reagents, imaging, biochemical/biomechanical stimulation and time points for the culture, which

ultimately influence the well-being of the system and effective analysis of the results[181]. An important design parameter is whether to have a direct or in-direct co-culture. A direct contact culture provides physical interactions and allows better signaling among cells however, diverse and heterogeneous cell environment may hinder analysis in identification of specific contributions to a process. Given that our system aims to analyze overall structure rather than specific interactions, an indirect method would not be suitable due to it lacks physical receptor-mediated cell-cell interactions[182]. However, such a system is influenced by parameters including cell types, seeding, density ratio of the cell types and culture medium compositions. In our system, initially mouse bone marrow was extracted and cultured as whole. As reported by Huang *et al.*, complete culturing of the bone marrow can allow obtaining high MSCs numbers[167]. In agreement with the article, after 14 days of culture we observed spindle-shaped cells and as the cells were passaged the number increased significantly (Fig. 19) Additionally, the same protocol suggested that as the passage number increases the monocyte/macrophage number in the culture would decrease. Therefore, we decided to use an earlier passage than suggested to obtain both MSCs and monocyte/macrophages. The initial flow analysis of freshly isolated BM cells confirmed that the protocol is able to provide both mesenchymal and monocytic cell types (Fig. 21). This allowed a single step culture for obtaining cells both for osteoblast and osteoclast differentiation. Moreover, after the third passage, the cultured population was subjected to flow cytometry analysis. It was observed that the numbers of both cell types were increased in the cultured populations (Fig. 22). In order to evaluate the osteogenic differential potential of MSCs, alizarin red staining carried out. Calcium deposition on ECM has been observed, supporting the presence of osteogenic cells differentiation (Fig. 25). Finally, qPCR analysis after 21 days of differentiation showed that ALP, cathepsin K and osteocalcin levels were significantly increased (Fig. 23).

Using a femur head for positive control allowed a comparison between the dynamically cultured engineered scaffold and native environment (Fig. 27). Although the engineered system consists of only mesenchymal and monocytic cells that were cultured and differentiated for 21 days, several similarities such as cellular morphology, ECM secretion and cell-cell interactions were observed. An important indication of favorable environment was the ECM secretion. As the positive control shows a dense ECM structure covering almost all surfaces, the engineered

scaffold showed a similar structure. Moreover, in a similar manner, cellular extensions cover large areas forming junctions between cells and a web-like structure can be observed (Fig. 32).

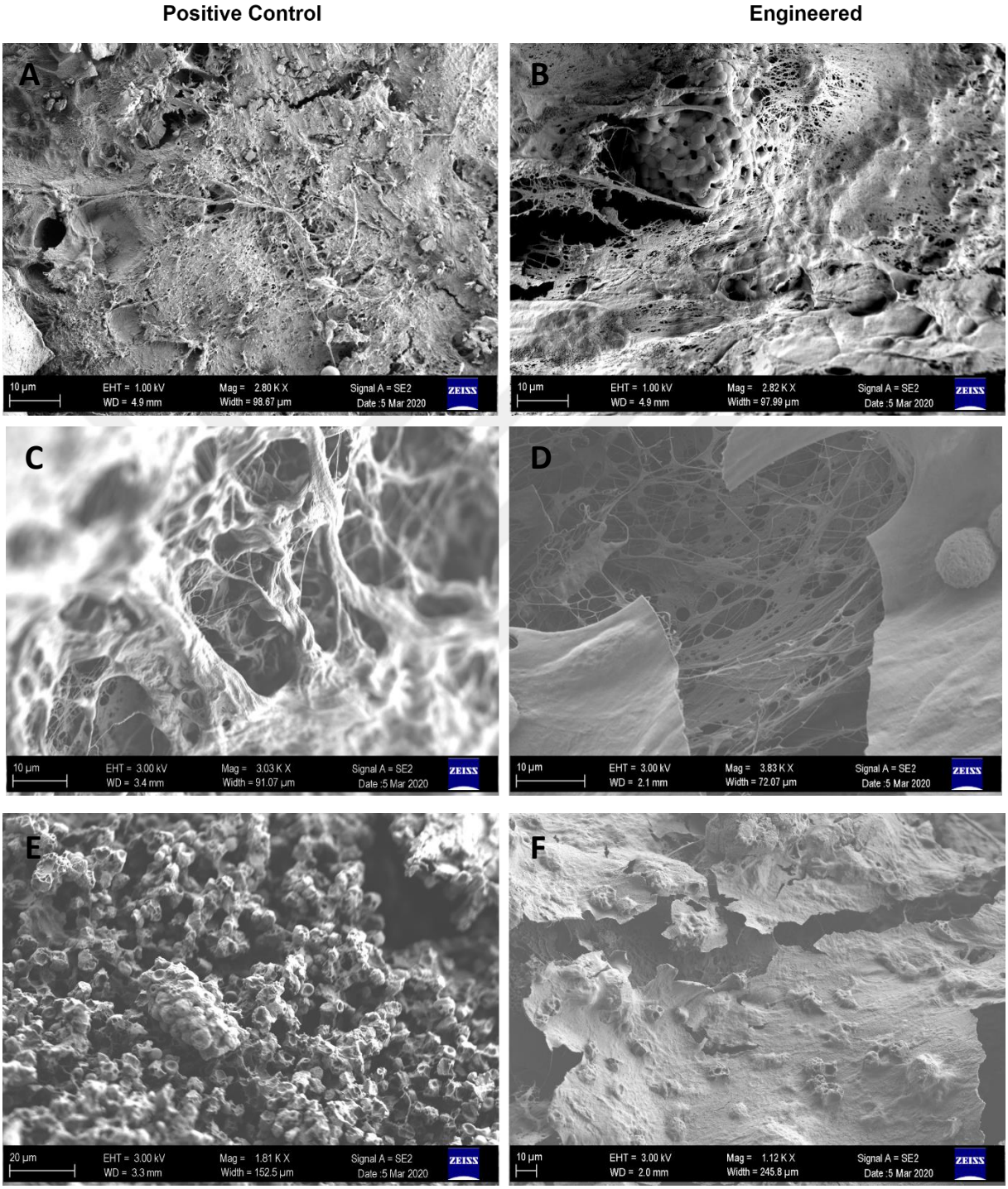

Figure 32. Comparison of dynamically cultured engineered scaffold with mouse femur head. (A-D) The engineered structure highly resembles native environment in terms of ECM formation. (E-F) Although cellular density of the native bone is higher, engineered cell structure is highly mimicry.

As *in vivo* methods often bring ethical considerations; *in vitro* models using primary cells may represent a valid alternative. Moreover, basic mechanisms in both healthy and diseased bone states can be recreated using 3D dynamic methods. Current advances in *in silico* models and imaging modalities can enhance the models and may allow fine-tuning in parameters. Finally, additional counterparts including macrophages and angiogenic processes have been identified and can be adopted in such studies.

In conclusion, co-culturing cells allow a deeper exploration of cellular interaction and offer a replica of naturally occurring processes in miniaturized mimicries, which can bring novel methods and help developing reliable bone organ models. An optimal 3D co-culture protocol for bone tissue cells to accurately model the microenvironment is currently lacking, however, a plethora of data is available which can be helpful.

6 CONCLUSION AND FUTURE PERSPECTIVES

The goal of this thesis was to develop a co-culture system with a tailored bioceramic that can be used in bioreactors to model bone microenvironment. The flow cytometry analysis indicated that after *in vitro* culture period of primary mBM cells both MSCs and MØ phenotype cells were present. Together, these cells can differentiate into osteoblasts and osteoclasts and form basic bone microenvironment. This finding is supported with the higher expression levels of ALP, cathepsin-K and osteocalcin levels after the culture period. However, in order to create a functional an accurate model, the system requires much more than the co-culture of these cell types. ß-TCP is a resorbable bioceramic with osteoconductive and osteoinductive capabilities. Tailoring this ceramic in terms of thickness and porosity may help for such a system. The SEM analysis showed a complete ECM formation on the surface and inner structure after 3 weeks of dynamic culture. Our cell-seeded scaffold can be implemented into different types of bioreactors with differently shaped chambers.

Although this study can be used to create a tailored cell-scaffold environment, the dynamic culturing parameters such as flow rate and shear stress are not covered. Thus, further investigations must be made to fully understand the effect of such parameters in this system.

Moreover, the system can be used to model a mathematical simulation to calculate stress and strain distribution, fluid shear stress and scaffold properties to form a realistic view to studies. Further, most studies include an *in vivo* trial to confirm the data, which may require consideration of endothelial cells for the formation of vascular network and increase cell viability on scaffolds upon implantation.

Another aspect that can be considered is to design an *in situ* environment by incorporating sensors such as O_2 and pH sensors to simultaneously determine the physiological changes in the system without the need of experimentation that may require extensive invasive cellular and histologic analysis. Moreover, addition of mechanical actuators to the system may allow better mimicking of the bone environment.

7 REFERENCES

[1] G. J. Meijer, J. D. De Bruijn, R. Koole, and C. A. Van Blitterswijk, "Cell-based bone tissue engineering," *PLoS Med.*, 2007.

[2] A. M. Yousefi, P. F. James, R. Akbarzadeh, A. Subramanian, C. Flavin, and H. Oudadesse, "Prospect of stem cells in bone tissue engineering: A review," *Stem Cells International*. 2016.

[3] S. Bose, M. Roy, and A. Bandyopadhyay, "Recent advances in bone tissue engineering scaffolds," *Trends in Biotechnology*. 2012.

[4] P. Zhao, H. Gu, H. Mi, C. Rao, J. Fu, and L. sheng Turng, "Fabrication of scaffolds in tissue engineering: A review," *Frontiers of Mechanical Engineering*. 2018.

[5] M. I. Gariboldi and S. M. Best, "Effect of ceramic scaffold architectural parameters on biological response," *Frontiers in Bioengineering and Biotechnology*. 2015.

[6] F. Berthiaume, T. J. Maguire, and M. L. Yarmush, "Tissue Engineering and Regenerative Medicine: History, Progress, and Challenges," *Annu. Rev. Chem. Biomol. Eng.*, 2011.

[7] S. Caddeo, M. Boffito, and S. Sartori, "Tissue engineering approaches in the design of healthy and pathological in vitro tissue models," *Frontiers in Bioengineering and Biotechnology*. 2017.

[8] R. M. Klar, "The induction of bone formation: The translation enigma," *Frontiers in Bioengineering and Biotechnology*. 2018.

[9] A. J. Salinas, P. Esbrit, and M. Vallet-Regí, "A tissue engineering approach based on the use of bioceramics for bone repair," *Biomaterials Science*. 2013.

[10] Y. Chen *et al.*, "Enhanced effect of β-tricalcium phosphate phase on neovascularization of porous calcium phosphate ceramics: In vitro and in vivo evidence," *Acta Biomater.*, 2015.

[11] S. V. Dorozhkin, "Bioceramics of calcium orthophosphates," *Biomaterials*. 2010.

[12] S. V. Dorozhkin, "Calcium orthophosphates as bioceramics: State of the art," *Journal of Functional Biomaterials*. 2010.

[13] S. V. Dorozhkin, "Biphasic, triphasic and multiphasic calcium orthophosphates," *Acta Biomaterialia*. 2012.

[14] G. Velve-Casquillas, M. Le Berre, M. Piel, and P. T. Tran, "Microfluidic tools for cell biological research," *Nano Today*. 2010.

[15] C. F. Dewey, S. R. Bussolari, M. A. Gimbrone, and P. F. Davies, "The dynamic response of vascular endothelial cells to fluid shear stress," *J. Biomech. Eng.*, 1981.

[16] P. J. Lee, T. A. Gaige, and P. J. Hung, "Dynamic cell culture: A microfluidic function generator for live cell microscopy," *Lab Chip*, 2009.

[17] E. Leclerc *et al.*, "Study of osteoblastic cells in a microfluidic environment," vol. 27, pp.

586–595, 2006.

[18] C. Luni, E. Serena, and N. Elvassore, “Human-on-chip for therapy development and fundamental science,” *Current Opinion in Biotechnology*. 2014.

[19] Z. Wang, R. Samanipour, K. I. Koo, and K. Kim, “Organ-on-a-chip platforms for drug delivery and cell characterization: A review,” *Sensors Mater.*, 2015.

[20] A. U. R. Aziz, C. Geng, M. Fu, X. Yu, K. Qin, and B. Liu, “The role of microfluidics for organ on chip simulations,” *Bioengineering*. 2017.

[21] H. Avci, F. D. Güzel, S. Erol, and A. Akpek, “Recent advances in organ-on-a-chip technologies and future challenges: a review,” *Turkish J. Chem.*, 2018.

[22] N. Convery and N. Gadegaard, “30 years of microfluidics,” *Micro and Nano Engineering*. 2019.

[23] N. K. Inamdar and J. T. Borenstein, “Microfluidic cell culture models for tissue engineering,” *Current Opinion in Biotechnology*. 2011.

[24] H. Andersson and A. Van Den Berg, “Microfabrication and microfluidics for tissue engineering: State of the art and future opportunities,” *Lab on a Chip*. 2004.

[25] N. W. Choi, M. Cabodi, B. Held, J. P. Gleghorn, L. J. Bonassar, and A. D. Stroock, “Microfluidic scaffolds for tissue engineering,” *Nat. Mater.*, 2007.

[26] J. M. Seong, B. C. Kim, J. H. Park, I. K. Kwon, A. Mantalaris, and Y. S. Hwang, “Stem cells in bone tissue engineering,” *Biomedical Materials*. 2010.

[27] E. Jover, M. Fagnano, G. Angelini, and P. Madeddu, “Cell Sources for Tissue Engineering Strategies to Treat Calcific Valve Disease,” *Frontiers in Cardiovascular Medicine*. 2018.

[28] C. Colnot, “Cell sources for bone tissue engineering: Insights from basic science,” *Tissue Engineering - Part B: Reviews*. 2011.

[29] A. Khademhosseini *et al.*, “Embryonic Stem Cells as a Cell Source for Tissue Engineering,” in *Principles of Tissue Engineering: Fourth Edition*, 2013.

[30] J. O. Hollinger, T. A. Einhorn, B. A. Doll, and C. Sfeir, *Bone tissue engineering*. 2004.

[31] D. W. Hutmacher and A. J. Garcia, “Scaffold-based bone engineering by using genetically modified cells,” *Gene*. 2005.

[32] C. Heinemann, S. Heinemann, H. Worch, and T. Hanke, “Development of an osteoblast/osteoclast co-culture derived by human bone marrow stromal cells and human monocytes for biomaterials testing,” *Eur. Cells Mater.*, 2011.

[33] C. Correia *et al.*, “In vitro model of vascularized bone: Synergizing vascular development and osteogenesis,” *PLoS One*, 2011.

[34] P. M. Le, M. Andreeff, and V. Lokesh Battula, “Osteogenic niche in the regulation of normal hematopoiesis and leukemogenesis,” *Haematologica*. 2018.

[35] P. Bianco, “Bone and the hematopoietic niche: A tale of two stem cells,” *Blood*. 2011.

[36] S. J. Morrison and D. T. Scadden, “The bone marrow niche for haematopoietic stem cells,” *Nature*. 2014.

[37] D. B. Burr and O. Akkus, “Bone Morphology and Organization,” in *Basic and Applied Bone Biology*, 2013.

[38] R. Florencio-Silva, G. R. D. S. Sasso, E. Sasso-Cerri, M. J. Simões, and P. S. Cerri, “Biology of Bone Tissue: Structure, Function, and Factors That Influence Bone Cells,” *BioMed Research International*. 2015.

[39] J. C. Crockett, M. J. Rogers, F. P. Coxon, L. J. Hocking, and M. H. Helfrich, “Bone remodelling at a glance,” *J. Cell Sci.*, 2011.

[40] D. J. Hadjidakis and I. I. Androulakis, “Bone remodeling,” in *Annals of the New York Academy of Sciences*, 2006.

[41] R. Caudarella, F. Vescini, A. Buffa, E. Rizzoli, L. Ceccoli, and C. M. Francucci, “Role of calcium-sensing receptor in bone biology.,” *Journal of endocrinological investigation*. 2011.

[42] S. Y. Hwang and J. W. Putney, “Calcium signaling in osteoclasts,” *Biochimica et Biophysica Acta - Molecular Cell Research*. 2011.

[43] B. F. Boyce, E. Rosenberg, A. E. de Papp, and L. T. Duong, “The osteoclast, bone remodelling and treatment of metabolic bone disease,” *European Journal of Clinical Investigation*. 2012.

[44] R. M. Klar, R. Duarte, T. Dix-Peek, C. Dickens, C. Ferretti, and U. Ripamonti, “Calcium ions and osteoclastogenesis initiate the induction of bone formation by coral-derived macroporous constructs,” *J. Cell. Mol. Med.*, 2013.

[45] N. Rucci, “Molecular biology of bone remodelling,” *Clinical Cases in Mineral and Bone Metabolism*. 2008.

[46] N. Kohli *et al.*, “Bone remodelling in vitro: Where are we headed?: -A review on the current understanding of physiological bone remodelling and inflammation and the strategies for testing biomaterials in vitro,” *Bone*. 2018.

[47] J. S. Kenkre and J. H. D. Bassett, “The bone remodelling cycle,” *Annals of Clinical Biochemistry*. 2018.

[48] Y. Xie, Y. Chen, L. Zhang, W. Ge, and P. Tang, “The roles of bone-derived exosomes and exosomal microRNAs in regulating bone remodelling,” *Journal of Cellular and Molecular Medicine*. 2017.

[49] P. Katsimbri, “The biology of normal bone remodelling,” *European Journal of Cancer Care*. 2017.

[50] M. Prideaux, D. M. Findlay, and G. J. Atkins, “Osteocytes: The master cells in bone remodelling,” *Current Opinion in Pharmacology*. 2016.

[51] Encyclopaedia Britannica, “Bone remodeling.” [Online]. Available: https://www.britannica.com/science/bone-remodeling. [Accessed: 30-Mar-2020].

[52] R. Lanza, R. Langer, and J. P. Vacanti, *Principles of Tissue Engineering: Fourth Edition*.

2013.

[53] R. Langer and J. P. Vacanti, “Tissue engineering,” *Science (80-.).*, 1993.

[54] Y. Ikada, “Challenges in tissue engineering,” *Journal of the Royal Society Interface*. 2006.

[55] F. Akter, “Principles of Tissue Engineering,” in *Tissue Engineering Made Easy*, 2016.

[56] B. J. Huang, J. C. Hu, and K. A. Athanasiou, “Cell-based tissue engineering strategies used in the clinical repair of articular cartilage,” *Biomaterials*. 2016.

[57] M. J. Webber, O. F. Khan, S. A. Sydlik, B. C. Tang, and R. Langer, “A Perspective on the Clinical Translation of Scaffolds for Tissue Engineering,” *Ann. Biomed. Eng.*, 2015.

[58] M. Parmaksiz, A. Dogan, S. Odabas, A. E. Elçin, and Y. M. Elçin, “Clinical applications of decellularized extracellular matrices for tissue engineering and regenerative medicine,” *Biomed. Mater.*, 2016.

[59] E. A. Makris, A. H. Gomoll, K. N. Malizos, J. C. Hu, and K. A. Athanasiou, “Repair and tissue engineering techniques for articular cartilage,” *Nature Reviews Rheumatology*. 2015.

[60] B. K. Jong, R. Stein, and M. J. O’Hare, “Three-dimensional in vitro tissue culture models of breast cancer - A review,” *Breast Cancer Research and Treatment*. 2004.

[61] K. M. Yamada and E. Cukierman, “Modeling Tissue Morphogenesis and Cancer in 3D,” *Cell*. 2007.

[62] A. Mathur, Z. Ma, P. Loskill, S. Jeeawoody, and K. E. Healy, “In vitro cardiac tissue models: Current status and future prospects,” *Advanced Drug Delivery Reviews*. 2016.

[63] L. G. Griffith and M. A. Swartz, “Capturing complex 3D tissue physiology in vitro,” *Nature Reviews Molecular Cell Biology*. 2006.

[64] A. M. Hopkins, E. DeSimone, K. Chwalek, and D. L. Kaplan, “3D in vitro modeling of the central nervous system,” *Progress in Neurobiology*. 2015.

[65] K. S. Vellonen *et al.*, “A critical assessment of in vitro tissue models for ADME and drug delivery,” *Journal of Controlled Release*. 2014.

[66] Y. Peck and D. A. Wang, “Three-dimensionally engineered biomimetic tissue models for in vitro drug evaluation: Delivery, efficacy and toxicity,” *Expert Opinion on Drug Delivery*. 2013.

[67] N. T. Elliott and F. Yuan, “A review of three-dimensional in vitro tissue models for drug discovery and transport studies,” *Journal of Pharmaceutical Sciences*. 2011.

[68] L. Kimlin, J. Kassis, and V. Virador, “3D in vitro tissue models and their potential for drug screening,” *Expert Opinion on Drug Discovery*. 2013.

[69] J. C. Bernhard and G. Vunjak-Novakovic, “Should we use cells, biomaterials, or tissue engineering for cartilage regeneration?,” *Stem Cell Research and Therapy*. 2016.

[70] F. Khan and M. Tanaka, “Designing smart biomaterials for tissue engineering,” *Int. J. Mol. Sci.*, 2018.

[71] T. J. Keane and S. F. Badylak, “Biomaterials for tissue engineering applications,” *Semin. Pediatr. Surg.*, 2014.

[72] E. S. Place, N. D. Evans, and M. M. Stevens, “Complexity in biomaterials for tissue engineering,” *Nat. Mater.*, 2009.

[73] J. G. Nicholas, L. E. Watkins, and S. L. Voytik-Harbin, “Bone Tissue Engineering: Scalability and Optimization of Densified Collagen-Fibril Bone Graft Substitute Materials,” in *The Summer Undergraduate Research Fellowship (SURF) Symposium*, 2016.

[74] E. Roddy, M. R. DeBaun, A. Daoud-Gray, Y. P. Yang, and M. J. Gardner, “Treatment of critical-sized bone defects: clinical and tissue engineering perspectives,” *European Journal of Orthopaedic Surgery and Traumatology*. 2018.

[75] L. Roseti *et al.*, “Scaffolds for Bone Tissue Engineering: State of the art and new perspectives,” *Materials Science and Engineering C*. 2017.

[76] M. Bahraminasab and K. L. Edwards, “Biocomposites for Hard Tissue Replacement and Repair,” 2018.

[77] J. F. Bartolomé, J. S. Moya, R. Couceiro, C. F. Gutiérrez-González, F. Guitián, and A. Martinez-Insua, “In vitro and in vivo evaluation of a new zirconia/niobium biocermet for hard tissue replacement,” *Biomaterials*, 2016.

[78] B. Yuan, M. Zhu, and C. Y. Chung, “Biomedical porous shape memory alloys for hard-tissue replacement materials,” *Materials*. 2018.

[79] E. Mariani, G. Lisignoli, R. M. Borzì, and L. Pulsatelli, “Biomaterials: Foreign bodies or tuners for the immune response?,” *International Journal of Molecular Sciences*. 2019.

[80] M. Bohner, “Resorbable biomaterials as bone graft substitutes,” *Materials Today*. 2010.

[81] I. Bružauskaitė, D. Bironaitė, E. Bagdonas, and E. Bernotienė, “Scaffolds and cells for tissue regeneration: different scaffold pore sizes—different cell effects,” *Cytotechnology*. 2016.

[82] F. Gervaso, A. Sannino, and G. M. Peretti, “The biomaterialist’s task: scaffold biomaterials and fabrication technologies.,” *Joints*, vol. 1, no. 3, pp. 130–7, 2013.

[83] H. Qu, H. Fu, Z. Han, and Y. Sun, “Biomaterials for bone tissue engineering scaffolds: A review,” *RSC Advances*. 2019.

[84] E. F. Morgan, G. U. Unnikrisnan, and A. I. Hussein, “Bone Mechanical Properties in Healthy and Diseased States,” *Annu. Rev. Biomed. Eng.*, 2018.

[85] B. Mubeen, I. Ahmed, and A. Jameel, “Study of Mechanical Properties of Bones and Mechanics of Bone Fracture,” *Proc. 60th Congr. ISTAM*, 2016.

[86] D. D. Bosshardt, V. Chappuis, and D. Buser, “Osseointegration of titanium, titanium alloy and zirconia dental implants: current knowledge and open questions,” *Periodontology 2000*. 2017.

[87] T. Albrektsson, B. Chrcanovic, J. Mölne, and A. Wennerberg, “Foreign body reactions, marginal bone loss and allergies in relation to titanium implants,” *Eur. J. Oral Implantol.*,

2018.

[88] P. C. Banerjee, S. Al-Saadi, L. Choudhary, S. E. Harandi, and R. Singh, “Magnesium implants: Prospects and challenges,” *Materials*. 2019.

[89] T. Kraus *et al.*, “The influence of biodegradable magnesium implants on the growth plate,” *Acta Biomater.*, 2018.

[90] C. Sharma, A. K. Dinda, P. D. Potdar, C. F. Chou, and N. C. Mishra, “Fabrication and characterization of novel nano-biocomposite scaffold of chitosan-gelatin-alginate-hydroxyapatite for bone tissue engineering,” *Mater. Sci. Eng. C*, 2016.

[91] F. Fayyazbakhsh, M. Solati-Hashjin, A. Keshtkar, M. A. Shokrgozar, M. M. Dehghan, and B. Larijani, “Novel layered double hydroxides-hydroxyapatite/gelatin bone tissue engineering scaffolds: Fabrication, characterization, and in vivo study,” *Mater. Sci. Eng. C*, 2017.

[92] N. Celikkin, S. Mastrogiacomo, J. Jaroszewicz, X. F. Walboomers, and W. Swieszkowski, “Gelatin methacrylate scaffold for bone tissue engineering: The influence of polymer concentration,” *J. Biomed. Mater. Res. - Part A*, 2018.

[93] E. Sharifi *et al.*, “Preparation of a biomimetic composite scaffold from gelatin/collagen and bioactive glass fibers for bone tissue engineering,” *Mater. Sci. Eng. C*, 2016.

[94] M. Farokhi *et al.*, “Silk fibroin/hydroxyapatite composites for bone tissue engineering,” *Biotechnology Advances*. 2018.

[95] J. Melke, S. Midha, S. Ghosh, K. Ito, and S. Hofmann, “Silk fibroin as biomaterial for bone tissue engineering,” *Acta Biomaterialia*. 2016.

[96] Y. Wang, H. J. Kim, G. Vunjak-Novakovic, and D. L. Kaplan, “Stem cell-based tissue engineering with silk biomaterials,” *Biomaterials*. 2006.

[97] M. R. Sommer, J. R. Vetsch, J. Leemann, R. Müller, A. R. Studart, and S. Hofmann, “Silk fibroin scaffolds with inverse opal structure for bone tissue engineering,” *J. Biomed. Mater. Res. - Part B Appl. Biomater.*, 2017.

[98] S. Kuttappan, D. Mathew, and M. B. Nair, “Biomimetic composite scaffolds containing bioceramics and collagen/gelatin for bone tissue engineering - A mini review,” *Int. J. Biol. Macromol.*, 2016.

[99] C. Dhand *et al.*, “Bio-inspired in situ crosslinking and mineralization of electrospun collagen scaffolds for bone tissue engineering,” *Biomaterials*, 2016.

[100] A. M. Ferreira, P. Gentile, V. Chiono, and G. Ciardelli, “Collagen for bone tissue regeneration,” *Acta Biomaterialia*. 2012.

[101] C. M. Murphy, M. G. Haugh, and F. J. O’Brien, “The effect of mean pore size on cell attachment, proliferation and migration in collagen-glycosaminoglycan scaffolds for bone tissue engineering,” *Biomaterials*, 2010.

[102] Q. Yao *et al.*, “Design, construction and mechanical testing of digital 3D anatomical data-based PCL–HA bone tissue engineering scaffold,” *J. Mater. Sci. Mater. Med.*, 2015.

[103] W. Wang *et al.*, “Enhancing the hydrophilicity and cell attachment of 3D printed

PCL/graphene scaffolds for bone tissue engineering," *Materials (Basel).*, 2016.

[104] N. A. Pattanashetti, C. Hiremath, S. R. Naik, G. B. Heggannavar, and M. Y. Kariduraganavar, "Development of nanofibrous scaffolds by varying the TiO2 content in crosslinked PVA for bone tissue engineering," *New J. Chem.*, 2020.

[105] A. Satpathy *et al.*, "Bioactive Nano-Hydroxyapatite Doped Electrospun PVA-Chitosan Composite Nanofibers for Bone Tissue Engineering Applications," *Journal of the Indian Institute of Science*. 2019.

[106] J. R. Woodard *et al.*, "The mechanical properties and osteoconductivity of hydroxyapatite bone scaffolds with multi-scale porosity," *Biomaterials*, 2007.

[107] S. C. Cox, J. A. Thornby, G. J. Gibbons, M. A. Williams, and K. K. Mallick, "3D printing of porous hydroxyapatite scaffolds intended for use in bone tissue engineering applications," *Mater. Sci. Eng. C*, 2015.

[108] C. Zhou *et al.*, "Mechanical and biological properties of the micro-/nano-grain functionally graded hydroxyapatite bioceramics for bone tissue engineering," *J. Mech. Behav. Biomed. Mater.*, 2015.

[109] W. Habraken, P. Habibovic, M. Epple, and M. Bohner, "Calcium phosphates in biomedical applications: Materials for the future?," *Materials Today*. 2016.

[110] X. Xiao *et al.*, "The promotion of angiogenesis induced by three-dimensional porous beta-tricalcium phosphate scaffold with different interconnection sizes via activation of PI3K/Akt pathways," *Sci. Rep.*, 2015.

[111] Z. Chen, J. Yuen, R. Crawford, J. Chang, C. Wu, and Y. Xiao, "The effect of osteoimmunomodulation on the osteogenic effects of cobalt incorporated β-tricalcium phosphate," *Biomaterials*, 2015.

[112] J. R. Jones, L. M. Ehrenfried, and L. L. Hench, "Optimising bioactive glass scaffolds for bone tissue engineering," *Biomaterials*, 2006.

[113] L. C. Gerhardt and A. R. Boccaccini, "Bioactive glass and glass-ceramic scaffolds for bone tissue engineering," *Materials (Basel).*, 2010.

[114] Q. Fu, E. Saiz, M. N. Rahaman, and A. P. Tomsia, "Bioactive glass scaffolds for bone tissue engineering: State of the art and future perspectives," *Materials Science and Engineering C*. 2011.

[115] E. SCHEPERS, M. DE CLERCQ, P. DUCHEYNE, and R. KEMPENEERS, "Bioactive glass particulate material as a filler for bone lesions," *J. Oral Rehabil.*, 1991.

[116] J. Rauh, F. Milan, K. P. Günther, and M. Stiehler, "Bioreactor systems for bone tissue engineering," *Tissue Eng. - Part B Rev.*, 2011.

[117] J. Zhao, M. Griffin, J. Cai, S. Li, P. E. M. Bulter, and D. M. Kalaskar, "Bioreactors for tissue engineering: An update," *Biochemical Engineering Journal*. 2016.

[118] A. B. Yeatts and J. P. Fisher, "Bone tissue engineering bioreactors: Dynamic culture and the influence of shear stress," *Bone*. 2011.

[119] H. C. Chen and Y. C. Hu, "Bioreactors for tissue engineering," *Biotechnology Letters*.

2006.

[120] J. Yang *et al.*, “Proliferation and osteogenesis of immortalized bone marrow-derived mesenchymal stem cells in porous polylactic glycolic acid scaffolds under perfusion culture,” *J. Biomed. Mater. Res. - Part A*, 2010.

[121] H. Nokhbatolfoghahaei, M. R. Rad, M.-M. Khani, S. Shahriari, N. Nadjmi, and A. Khojasteh, “Application of Bioreactors to Improve Functionality of Bone Tissue Engineering Constructs: A Systematic Review,” *Curr. Stem Cell Res. Ther.*, 2017.

[122] D. Wendt, A. Marsano, M. Jakob, M. Heberer, and I. Martin, “Oscillating perfusion of cell suspensions through three-dimensional scaffolds enhances cell seeding efficiency and uniformity,” *Biotechnol. Bioeng.*, vol. 84, no. 2, pp. 205–214, 2003.

[123] E. Volkmer *et al.*, “Hypoxia in static and dynamic 3D culture systems for tissue engineering of bone,” *Tissue Eng. - Part A.*, 2008.

[124] J. F. Alvarez-Barreto, S. M. Linehan, R. L. Shambaugh, and V. I. Sikavitsas, “Flow perfusion improves seeding of tissue engineering scaffolds with different architectures,” *Ann. Biomed. Eng.*, 2007.

[125] F. W. Janssen, I. Hofland, A. Van Oorschot, J. Oostra, H. Peters, and C. A. Van Blitterswijk, “Online measurement of oxygen consumption by goat bone marrow stromal cells in a combined cell-seeding and proliferation perfusion bioreactor,” *J. Biomed. Mater. Res. - Part A*, 2006.

[126] G. N. Bancroft *et al.*, “Fluid flow increases mineralized matrix deposition in 3D perfusion culture of marrow stromal osteoblasts in a dose-dependent manner,” *Proc. Natl. Acad. Sci. U. S. A.*, 2002.

[127] H. L. Holtorf, T. L. Sheffield, C. G. Ambrose, J. A. Jansen, and A. G. Mikos, “Flow perfusion culture of marrow stromal cells seeded on porous biphasic calcium phosphate ceramics,” in *Annals of Biomedical Engineering*, 2005.

[128] H. L. Holtorf, J. A. Jansen, and A. G. Mikos, “Flow perfusion culture induces the osteoblastic differentiation of marrow stromal cell-scaffold constructs in the absence of dexamethasone,” in *Journal of Biomedical Materials Research - Part A*, 2005.

[129] M. E. Gomes, H. L. Holtorf, R. L. Reis, and A. G. Mikos, “Influence of the porosity of starch-based fiber mesh scaffolds on the proliferation and osteogenic differentiation of bone marrow stromal cells cultured in a flow perfusion bioreactor,” *Tissue Eng.*, 2006.

[130] M. E. Gomes, C. M. Bossano, C. M. Johnston, R. L. Reis, and A. G. Mikos, “In vitro localization of bone growth factors in constructs of biodegradable scaffolds seeded with marrow stromal cells and cultured in a flow perfusion bioreactor,” *Tissue Eng.*, 2006.

[131] L. Bjerre, C. E. Bünger, M. Kassem, and T. Mygind, “Flow perfusion culture of human mesenchymal stem cells on silicate-substituted tricalcium phosphate scaffolds,” *Biomaterials*, 2008.

[132] Y. Wang, T. Uemura, J. Dong, H. Kojima, J. Tanaka, and T. Tateishi, “Application of Perfusion Culture System Improves in Vitro and in Vivo Osteogenesis of Bone Marrow-Derived Osteoblastic Cells in Porous Ceramic Materials,” *Tissue Eng.*, 2003.

[133] N. E. Timmins, A. Scherberich, J. A. Früh, M. Heberer, I. Martin, and M. Jakob, "Three-dimensional cell culture and tissue engineering in a T-CUP (Tissue Culture under Perfusion)," *Tissue Eng.*, 2007.

[134] A. Papadimitropoulos *et al.*, "A 3D in vitro bone organ model using human progenitor cells," *Eur. Cells Mater.*, 2011.

[135] S. Gao, E. Şeker, and M. L. Yarmush, "Microfluidics: On-chip platforms as in vitro disease models," in *Microfluidic Technologies for Human Health*, 2012.

[136] P. S. Dittrich and A. Manz, "Lab-on-a-chip: Microfluidics in drug discovery," *Nature Reviews Drug Discovery*. 2006.

[137] B. H. Weigl, R. L. Bardell, and C. R. Cabrera, "Lab-on-a-chip for drug development," *Advanced Drug Delivery Reviews*. 2003.

[138] S. N. Bhatia and D. E. Ingber, "Microfluidic organs-on-chips," *Nature Biotechnology*. 2014.

[139] G. Pasirayi *et al.*, "Microfluidic Bioreactors for Cell Culturing: A Review," *Micro Nanosyst.*, 2012.

[140] Q. Zhou *et al.*, "Liver injury-on-a-chip: microfluidic co-cultures with integrated biosensors for monitoring liver cell signaling during injury," *Lab Chip*, 2015.

[141] N. D. Dinh *et al.*, "Microfluidic construction of minimalistic neuronal co-cultures," *Lab Chip*, 2013.

[142] A. D. Van Der Meer, V. V. Orlova, P. Ten Dijke, A. Van Den Berg, and C. L. Mummery, "Three-dimensional co-cultures of human endothelial cells and embryonic stem cell-derived pericytes inside a microfluidic device," *Lab Chip*, 2013.

[143] T. Bricks *et al.*, "Development of a new microfluidic platform integrating co-cultures of intestinal and liver cell lines," *Toxicol. Vitr.*, 2014.

[144] L. J. Chen *et al.*, "Microfluidic co-cultures of retinal pigment epithelial cells and vascular endothelial cells to investigate choroidal angiogenesis," *Sci. Rep.*, 2017.

[145] D. Patel *et al.*, "Microfluidic co-cultures with hydrogel-based ligand trap to study paracrine signals giving rise to cancer drug resistance," *Lab Chip*, 2015.

[146] H. Hwang, J. Park, C. Shin, Y. Do, and Y. K. Cho, "Three dimensional multicellular co-cultures and anti-cancer drug assays in rapid prototyped multilevel microfluidic devices," *Biomed. Microdevices*, 2013.

[147] R. Owen and G. C. Reilly, "In vitro models of bone remodelling and associated disorders," *Frontiers in Bioengineering and Biotechnology*. 2018.

[148] G. Borciani, G. Montalbano, N. Baldini, G. Cerqueni, C. Vitale-Brovarone, and G. Ciapetti, "Co–culture systems of osteoblasts and osteoclasts: Simulating in vitro bone remodeling in regenerative approaches," *Acta Biomaterialia*. 2020.

[149] A. Sieberath, E. Della Bella, A. M. Ferreira, P. Gentile, D. Eglin, and K. Dalgarno, "A comparison of osteoblast and osteoclast in vitro co-culture models and their translation for preclinical drug testing applications," *International Journal of Molecular Sciences*.

2020.

[150] K. Middleton, S. Al-dujaili, X. Mei, A. Günther, and L. You, “Microfluidic co-culture platform for investigating osteocyte-osteoclast signalling during fluid shear stress mechanostimulation,” *J. Biomech.*, vol. 59, pp. 35–42, 2017.

[151] P. Occhetta, R. Visone, and M. Rasponi, “High-throughput microfluidic platform for 3D cultures of mesenchymal stem cells,” in *Methods in Molecular Biology*, 2017.

[152] C. Wei *et al.*, “Osteocyte culture in microfluidic devices Osteocyte culture in microfluidic devices,” vol. 014109, 2015.

[153] T. B. Constructs, S. H. Cartmell, D. Ph, B. D. Porter, A. J. García, and D. Ph, “Effects of Medium Perfusion Rate on Cell-Seeded,” vol. 9, no. 6, pp. 1197–1203, 2003.

[154] A. Marturano-kruik, M. Maria, K. Yeager, A. Chramiec, L. Hao, and S. Robinson, “Human bone perivascular niche-on-a-chip for studying metastatic colonization,” 2017.

[155] S. Bersini *et al.*, “A microfluidic 3D invitro model for specificity of breast cancer metastasis to bone,” *Biomaterials*, 2014.

[156] S. H. Park, W. Y. Sim, B. H. Min, S. S. Yang, A. Khademhosseini, and D. L. Kaplan, “Chip-Based Comparison of the Osteogenesis of Human Bone Marrow- and Adipose Tissue-Derived Mesenchymal Stem Cells under Mechanical Stimulation,” *PLoS One*, 2012.

[157] Y. S. Torisawa *et al.*, “Bone marrow-on-a-chip replicates hematopoietic niche physiology in vitro,” *Nat. Methods*, vol. 11, no. 6, pp. 663–669, 2014.

[158] S. Sieber *et al.*, “Bone marrow-on-a-chip: Emulating the human bone marrow,” *bioRxiv*, 2018.

[159] N. Jusoh, S. Oh, S. Kim, J. Kim, and N. L. Jeon, “Microfluidic vascularized bone tissue model with hydroxyapatite-incorporated extracellular matrix,” *Lab Chip*, 2015.

[160] E. L. George, S. L. Truesdell, S. L. York, and M. M. Saunders, “Lab-on-a-chip platforms for quanti fi cation of multicellular interactions in bone remodeling,” *Exp. Cell Res.*, vol. 365, no. 1, pp. 106–118, 2018.

[161] C. Moraes, Y. Sun, and C. A. Simmons, “(Micro)managing the mechanical microenvironment,” *Integrative Biology*. 2011.

[162] S. Kou *et al.*, “A multishear microfluidic device for quantitative analysis of calcium dynamics in osteoblasts,” *Biochem. Biophys. Res. Commun.*, 2011.

[163] M. A. A. Muhamad Nor, L. C. Hong, Z. Arifin Ahmad, and H. Md Akil, “Preparation and characterization of ceramic foam produced via polymeric foam replication method,” *J. Mater. Process. Technol.*, 2008.

[164] Q. Chen, J. Roether, and A. Boccaccini, “Tissue Engineering Scaffolds from Bioactive Glass and Composite Materials,” *Top. Tissue Eng.*, 2008.

[165] H. Fu *et al.*, “In vitro evaluation of borate-based bioactive glass scaffolds prepared by a polymer foam replication method,” *Mater. Sci. Eng. C*, 2009.

[166] Q. Fu, M. N. Rahaman, B. Sonny Bal, R. F. Brown, and D. E. Day, “Mechanical and in vitro performance of 13-93 bioactive glass scaffolds prepared by a polymer foam replication technique,” *Acta Biomater.*, 2008.

[167] S. Huang, L. Xu, Y. Sun, T. Wu, K. Wang, and G. Li, “An improved protocol for isolation and culture of mesenchymal stem cells from mouse bone marrow,” *J. Orthop. Transl.*, 2015.

[168] M. Wagner *et al.*, “Isolation and intravenous injection of murine bone marrow derived monocytes,” *J. Vis. Exp.*, 2014.

[169] J. T. Y. Lee and K. L. Chow, “SEM sample preparation for cells on 3D scaffolds by freeze-drying and HMDS,” *Scanning*, 2012.

[170] S. A. González-Chávez, C. Pacheco-Tena, C. E. Macías-Vázquez, and E. Luévano-Flores, “Assessment of different decalcifying protocols on Osteopontin and Osteocalcin immunostaining in whole bone specimens of arthritis rat model by confocal immunofluorescence,” *Int. J. Clin. Exp. Pathol.*, 2013.

[171] S. Wu, X. Liu, K. W. K. Yeung, C. Liu, and X. Yang, “Biomimetic porous scaffolds for bone tissue engineering,” *Materials Science and Engineering R: Reports*. 2014.

[172] D. W. Hutmacher, J. T. Schantz, C. X. F. Lam, K. C. Tan, and T. C. Lim, “State of the art and future directions of scaffold-based bone engineering from a biomaterials perspective,” *J. Tissue Eng. Regen. Med.*, 2007.

[173] B. Stevens, Y. Yang, A. Mohandas, B. Stucker, and K. T. Nguyen, “A review of materials, fabrication methods, and strategies used to enhance bone regeneration in engineered bone tissues,” *Journal of Biomedical Materials Research - Part B Applied Biomaterials*. 2008.

[174] E. Saiz, E. A. Zimmermann, J. S. Lee, U. G. K. Wegst, and A. P. Tomsia, “Perspectives on the role of nanotechnology in bone tissue engineering,” *Dent. Mater.*, 2013.

[175] A. K. Born, M. Rottmar, S. Lischer, M. Pleskova, A. Bruinink, and K. Maniura-Weber, “Correlating cell architecture with osteogenesis: First steps towards live single cell monitoring,” *Eur. Cells Mater.*, 2009.

[176] E. D. F. Ker *et al.*, “Engineering spatial control of multiple differentiation fates within a stem cell population,” *Biomaterials*, 2011.

[177] S. Lamouille, J. Xu, and R. Derynck, “Molecular mechanisms of epithelial-mesenchymal transition,” *Nature Reviews Molecular Cell Biology*. 2014.

[178] T. J. Voegele *et al.*, “The effect of different isolation techniques on human osteoblast-like cell growth,” *Anticancer Res.*, 2000.

[179] E. Kylmäoja *et al.*, “Peripheral blood monocytes show increased osteoclast differentiation potential compared to bone marrow monocytes,” *Heliyon*, 2018.

[180] T. Suda, N. Udagawa, I. Nakamura, C. Miyaura, and N. Takahashi, “Modulation of osteoclast differentiation by local factors,” *Bone*, 1995.

[181] K. G. Battiston, J. W. C. Cheung, D. Jain, and J. P. Santerre, “Biomaterials in co-culture

systems: Towards optimizing tissue integration and cell signaling within scaffolds," *Biomaterials*. 2014.

[182] G. Il Im, "Coculture in musculoskeletal tissue regeneration," *Tissue Engineering - Part B: Reviews*. 2014.

[183] M. Haffner-Luntzer, A. Liedert, and A. Ignatius, "Mechanobiology of bone remodeling and fracture healing in the aged organism," *Innovative Surgical Sciences*. 2020.

[184] I. Martin, D. Wendt, and M. Heberer, "The role of bioreactors in tissue engineering," *Trends in Biotechnology*. 2004.

[185] H. Kimura, Y. Sakai, and T. Fujii, "Organ/body-on-a-chip based on microfluidic technology for drug discovery," *Drug Metabolism and Pharmacokinetics*. 2018.

[186] D. Huh, B. D. Matthews, A. Mammoto, M. Montoya-Zavala, H. Yuan Hsin, and D. E. Ingber, "Reconstituting organ-level lung functions on a chip," *Science (80-.).*, 2010.

[187] M. J. Powers *et al.*, "A microfabricated array bioreactor for perfused 3D liver culture," *Biotechnol. Bioeng.*, 2002.

[188] Y. Nakao, H. Kimura, Y. Sakai, and T. Fujii, "Bile canaliculi formation by aligning rat primary hepatocytes in a microfluidic device," *Biomicrofluidics*, 2011.

[189] K. J. Jang and K. Y. Suh, "A multi-layer microfluidic device for efficient culture and analysis of renal tubular cells," *Lab Chip*, 2010.

[190] C. P. Ng, Y. Zhuang, A. W. H. Lin, and J. C. M. Teo, " A Fibrin-Based Tissue-Engineered Renal Proximal Tubule for Bioartificial Kidney Devices: Development, Characterization and In Vitro Transport Study ," *Int. J. Tissue Eng.*, 2013.

[191] H. Kimura, T. Yamamoto, H. Sakai, Y. Sakai, and T. Fujii, "An integrated microfluidic system for long-term perfusion culture and on-line monitoring of intestinal tissue models," *Lab Chip*, 2008.

8 APPENDIX

8.1 *Ethic Committee Approval*

İZMİR BİYOTIP VE GENOM MERKEZİ
HAYVAN DENEYLERİ YEREL ETİK KURULU (İBG-HADYEK)
KARARI

Toplantı Tarihi	: 13/05/2020	**Toplantı Günü**	: Çarşamba
Toplantı Sayısı	: 7	**Toplantı Saati**	: 16:30

Sayın Doç. Sinan GÜVEN,

2020-018 Protokol No'lu; yürütücüsü olduğunuz "Mikroakışkan biyoreaktörlerde B-TCP esaslı doku iskeleleri kullanılarak osteojenik niş geliştirilmesi" başlıklı projenin uygulanmasında etik açıdan sakınca olmadığına oy birliği ile karar verilmiştir.

Bilgilerinizi ve gereğini rica ederiz.

Doç. Dr. Güneş ÖZHAN BAYKAN **Başkan**	(Onayladı) **Vet. Hek. Kerem ESMEN** **Başkan Yardımcısı**
(Onayladı) **Prof. Dr. H. Alper BAĞRIYANIK** **Üye**	(Onayladı) **Prof. Dr. Ensari GÜNELİ** **Üye**
Doç. Dr. Kasım DİRİL **Üye (Katılmadı)**	(Onayladı) **Dr. Öğr. Üyesi Ayşe Banu DEMİR** **Üye**
Dr. Gülşin ÇAKAN AKDOĞAN **Üye (Katılmadı)**	(Onayladı) **Vet. Hek. Umur KELEŞ** **Üye**
(Onayladı) **H. Muammer KARAGÖZ** **Üye**	

8.2 Curriculum vitae

IBRAHIM HALILULLAH ERBAY

ID No / Passport No	29200491074
Date of Birth	24.06.1994
e-mail	halilullaherbay@gmail.com

EDUCATIONAL BACKGROUND

Country	University	Faculty/Institute	Department	Degree	Year of Graduation
Turkey	Dokuz Eylul University	Izmir International Biomedicine And Genome Institute	Molecular Biology and Genetics	Master of Science	2020
Turkey	Manisa Celal Bayar University	Faculty of Engineering	Metallurgical and Material Engineering	Bachelor	2018
Turkey	Manisa Celal Bayar University	Faculty of Engineering	Bioengineering	Bachelor	2018

ACADEMIC / PROFESSIONAL EXPERIENCE

University	Country	City	Unit	Position	Year
Newcastle University	UK	Newcastle	Chemical Engineering and Advanced Materials	Intern	2015
Politecnico di Milano	Italy	Milano	Dipartimento di Elettronica, Informazione e Bioingegneria	Intern	2018

Specialized Field
Tissue engineering Biomaterials Microfluidic Systems Molecular Biology and Genetics

CONFERENCES and AWARDS

Oral Presentation: Erbay HI., Karaman O., Guven S. (2020). Microfluidic Bone Organ, TERMIS-EU 2020, Manchester, 26-29 May. (Accepted)
Poster Presentation: Erbay HI., Karaman O., Guven S. (2019). Osteogenic Niche Under Dynamic Culture Conditions with Microfluidic Bioreactors, BIOMED2019. Biomedical Science and Technology Symposium, İzmir, 17-20 October
Oral Presentation: Erbay HI., Karaman O., Guven S. (2018). Developing 3D Printed Scaffold Masters for Microfluidic Bioreactors, International Symposium on 3D Printing in Medicine, Ankara, 16-17 November
Poster Presentation: Erbay HI., Karaman O., Guven S. (2018). Mikroakıskan Biyoreaktörlere Yönelik Osteojenik Taşıyıcı İskele Geliştirilmesi, BIOMED2018-TR, İstanbul, 15-16 December
Finalist Award at Turkish Airlines 7th Science Expo (2018).
2nd place in Manisa Celal Bayar University 26th Science Expo-Engineering Category (2018).

PUBLICATIONS

Erbay, HI., Baş, A., **Asal, M.**, Yanık, H., Güven, S. (2018). Mikroakışkan Sistemler ve Doku Mühendisliği. Palme Yayınları.